NTNU

Norwegian University of
Science and Technology

Study on the Variable Frequency Transformer's Operation and Frequency Range

Kooshiar Nasrollahi

Master thesis
Supervisor: Professor Olimpo Anaya-Lara
Trondheim, March 2022

Department of Electric Power Engineering
Faculty of Information Technology and Electrical Engineering
Norwegian University of Science and Technology

Abstract

Inherently variable power generation from renewable energy sources (RES), such as wind turbines and solar panels, is challenging for energy shifting. Merging separated power grids into a super grid with various RES besides the different peak times and seasons in distinct regions help to overcome the RES fluctuations. The variable frequency transformer (VFT) asynchronous grids interconnection offers flexible power flow between different areas, developing power grids' reliability and balancing mismatches in supply and demand in an area.

The recent shift from conventional synchronous power generation plants to wind power and PVs reduces power systems' frequency stability. Increasing full-converter wind turbines, which isolate the generator rotational speed from the grid frequency, decreases the power system's physical inertia. PV power plants also miss any physical inertia. Physical inertia is vital in the early stage of the frequency disturbances for power systems' stability. General power systems' frequency droop characteristic suggests that employing a VFT, which has significantly high inertia constant, improves the power system's frequency stability. Also, the VFT fundamental structure offers frequency ancillary service in frequency transient of rotor swing, stage I, inertial frequency drop, stage II, primary control, stage III, and secondary control, stage IV. Utilising the VFT interconnection with energy storage banks (ESB) show similar dynamics to a synchronous generator. The VFT bidirectional power transfer capability contributes to both over and under power mismatch.

This study reviewed the VFT operating and power systems' frequency transient response to analysing the VFT behaviour during the frequency shifting operation and possible involvement in inertial, primary and secondary frequency control. The VFT behaviour is analysed and tested in the MATLAB\Simulink. This study focuses on the maximum possible active power transmission during frequency shifting and the VFT's frequency drop characteristic during a frequency disturbance.

Preface

This report represents the master's thesis study for graduating in power system operation and analysis at the electric power engineering department of the Norwegian University of Science and Technology. This study performed based on the author's pre-work *'Modelling and Analysis of a Rotary Transformer for Power Take-off System of an X-Rotor Wind Turbine'* [1] to cover defined future works and investigate some other potential application of the Variable Frequency Transformer in power systems.

I would like to thank my supervisor, Professor Olimpo Anaya-Lara at the University of Strathclyde, Glasgow, and NTNU, for his strong knowledge and professional support, which gave me great inspiration to carry out the study and led through the project.

Trondheim, March 2022,

Kooshiar Nasrollahi

Table of Contents

List of Figures

List of Tables

List of Abbreviations

AC Alternating Current

DC Direct Current

DES Distributed Energy Source

DFIG Doubly Fed Induction Generator

ESB Energy Storage Bank

FACTS Flexible AC Transmission System

FASAL Flexible Asynchronous AC Link

HAWT Horizontal Axis Wind Turbine

HVAC High Voltage AC

HVDC High Voltage DC

LCC-HVDC Line Commutated Converter HVDC

LFAC Low Frequency AC

LFEO Low-Frequency Electromechanical Oscillations

MMC-HVDC Modular Multilevel Converter HVDC

MVC Main VFT Control System

OWF Offshore Wind Farm

PCC Point of Common Connection

PF Power Factor

PLL Phase Locked Loop

PMS/EMS Power and Energy Management System

PMSG Permanent Magnet Synchronous Generator

PV Photovoltaics

RES Renewable Energy Sources

RoCoF Rate of Change of Frequency

RT Rotary Transformer

SCR Short Circuit Ratio

UVC Unit VFT Control System

VAWT Vertical Axis Wind Turbine

VFT Variable Frequency Transformer

VSC-HVDC Voltage Source Converter HVDC

WRIM Wound Rotor Induction Machine

Chapter 1

Introduction

This chapter gives an introduction to the conducted study and the report. It describes the motivations of the performed work based on the explained background studies and clarifies the followed objectives considering the defined study goal. It also determines the used methods and scope of the analysis. The last section depicts the report structure.

1.1 Background and Motivation

The initial motivation for investigating the variable frequency transformer (VFT) comes from the [1]. The proposed power take-off system for the offshore X-rotor wind turbine transfer the generated power from the two secondary rotors from the main rotor by the 3-phase rotary transformer (RT) to the stationary part of the turbine. Still, the inherent fluctuations in the X-rotor power take-off frequency, according to sinusoidal effective wind speed on the second rotors, even in the constant wind profile with a direct mechanical power drive in the X-rotor[2], requires a frequency flatter for increasing the generated power quality.

At the same time, [3] suggested the low-frequency AC (LFAC) power transmission method implementation in the offshore wind power to support in two main areas. The first advantage of the LFAC is reducing the wind turbines' gear ratio and allowing the more simple and lighter design of offshore wind turbines and, consequently, cheaper offshore wind turbines both in capital and installation costs. It is mainly because of the low revolution speed of the giant wind turbines. The LFAC technology also supports a higher power transmission capacity in the high voltage AC (HVAC) links and a longer distance of up to 160(km) [6]. Recent research suggests the technical and economic benefits of the LFAC technology in the offshore wind power transfer over certain distances [4]. It could also propose a lower energy cost from the offshore wind farms by eliminating the radical offshore converter substations of the high voltage DC (HVDC) links, and their frequent maintenance requirement costs [5]. However, LFAC suffers from the massive transformers volume requirement due to the low-frequency operation. The LFAC transformers have three times greater core cross-section than the usual 50 (Hz) operating transformers. The VFT capability for frequency shifting that [1] reviewed to some extent also encourages the study of the VFT behaviour in the LFAC power transmission system.

The primary motivation and concern for the master's degree study final project are renewable energy sources (RES) development, which is becoming more vital due to the carbon emission crisis. Still, inherently variable power generation of RES, such as wind turbines and solar panels, is a challenge for energy shifting. The recent shift from conventional synchronous power generation plants to wind power and PVs reduces power systems' frequency stability. Increasing full-converter wind turbines, which isolate the generator rotational speed from the grid frequency, decreases the power system's physical inertia. PV power plants also miss any physical inertia. Physical inertia is vital in the early stage of the frequency disturbances for power systems' frequency recovery. Some research evaluates introducing synthetic inertia impact on the small disturbances [47] and large disturbances frequencyserv3 frequency recovery and show improvement in the rate of change of frequency (RoCoF) with improving inertia constant of the power plant seen by the grid. Also, a recent study proposes new concepts for improving offshore wind farms (OWF) frequency ancillary services with synchronous generator support on the shore side of OWFs PCC tie-in[15]. [16] examine energy storage banks (ESB) power reserve impact on the frequency response of the close connected OWF. General power systems' frequency droop characteristic shows that employing a VFT, which has significantly high inertia constant, improves the power system's frequency response. Utilising the VFT interconnection with ESBs show similar dynamics of a synchronous generator on the OWF PCC tie-in, which

can help the OWF frequency response. It introduces physical inertia inherently to improve the RoCoF. It also responds to frequency disturbances automatically, such as a synchronous power plant without any frequency measurement instrument requirement. It also supports bidirectional power transfer that contributes to both over and under power mismatch. It delivers power from the ESB in dropping frequency events and charges the ESB to prevent the frequency by power surplus. In such a configuration, the VFT combined with ESB supports the primary and secondary frequency control and facilitates the near OWF's frequency response improvement.

The general configuration and brief concept of the VFT system asynchronous interconnection are described in the following. This study follows this configuration and the shown power flow direction in all analyses, test system development, and examined applications.

1.1.1 VFT Asynchronous Interconnection

VFT technology was developed and commercialised for the first time in the early 2000s by General Electric Company. Four other VFTs were installed and operated only in the next six years, considering their advantage over the other available technologies. Considering VFT's vast functionalities, it will play an essential role in future global power exchange capacity and help grid operators with more flexible interconnected power systems. VFT has included a wound rotor induction machine (WRIM) as a rotary transformer (RT) and rotor control drive by a DC motor. The RT provides bi-directional power flow between connected power grids to the VFT's stator and rotor through the air gap flux and compensates the connected power grids' frequency difference by a continuous rotating rotor. The rotor control drive regulates power flow's direction and magnitude by the applied torque on the RT's rotor through the mechanically coupled DC motor shaft. Figure 1.1 depicts the VFT asynchronous interconnection configuration and the power flows direction this study is based on. In this study, the $g1$ and $g2$ subscripts are used as respectively stator and rotor side connected power grids.

1.2 Problem Definition

VFT stands as a promising technology for asynchronous power grid tie-in, considering the represented comparison in AsynchTech. Also, frequency matching function in the X-rotor power take-off system, LFAC system and introducing frequency control ancillary service raises the VFT behaviour study in a wide range frequency shifting function, inquiry. Increasing frequency shifting increases the WRIM operating slip that impacts the VFT systems' efficiency negatively by increasing the DC motor's power requirement for frequency matching[29].

Besides that, uncontrollable reactive power flow through the VFT also occupies the VFT windings and tie-in line capacity. It negatively affects possible active power transfer, grids' voltages,

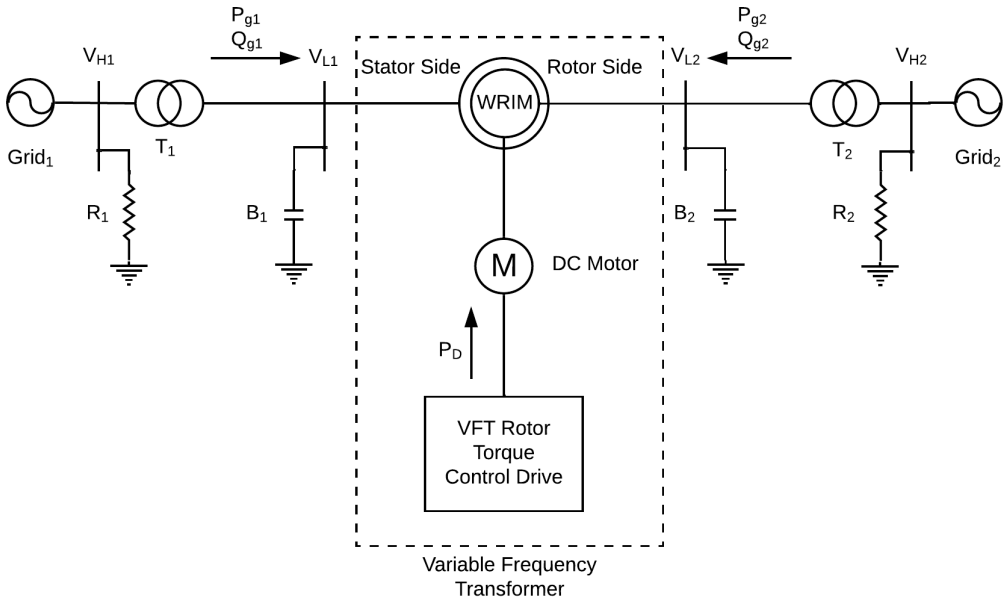

Figure 1.1: The studied asynchronous VFT interconnection configuration single-line diagram.

system stability and generally power quality. In this manner, a comprehensive study of VFT's reactive power behaviour in asynchronous interconnections with a wide range of frequency shifting is essential. This study focuses mainly on specifying the VFT reactive power characteristics and maximum possible active power transfer.

Proposing the VFT system for power systems' frequency ancillary service as a synchronous power plant requires studying and understanding the VFT dynamic response and analysing its frequency droop characteristic. Also, developing a test system that analyses the frequency response of the VFT supports future research.

1.3 Objectives

Regarding the defined study's primary aim to investigate the VFT behaviour during the wide range frequency matching and the frequency ancillary service potential by the VFT, the study's objectives are divided into three parts.

Create a concrete theory understanding
Understand the VFT system concept and operating theory, available control and protection schemes for the various operating situations of the VFT. To support further analysis, provide an analytical study of the VFT system for the frequency matching operation. Review the power

systems' general frequency characteristics, and study the primary and secondary frequency regulation in synchronous power plants. Analyse the VFT system in frequency disturbances according to the power system dynamics.

Develop a VFT asynchronous interconnection test system.
Build the VFT interconnection model based on the learned theory and implement the suggested control strategies required for frequency matching and dynamic response studies. Validate the developed model with available scientific research and analytical studies.

Determine the VFT reactive power flow behaviour during frequency matching and dynamic response to frequency disturbances.
In different operating scenarios, the test system and analytical studies investigate the VFT reactive power flow characteristic, maximum possible active power transfer, system stability, and power quality. The different studied scenarios evaluate the VFT system operating limits.

1.4 Methodology

Literature review starts the study to understand the concept and fundamental operating theory of the VFT and power systems' frequency regulations. It also assembles the required knowledge of the frequency matching operating and disturbances response to define investigating scenarios condition and required parameters. Reviewing the WRIM theories supports the analytical studies and simulation results analysis. In the lack of a pre-available model for a VFT system, the test system is developed from scratch in Matlab\Simulink with the specialised power system from the Simscape library. Matlab also manages analytical studies and simulation results for a comprehensive comparison and presentation.

1.5 Scope and Assumption

The VFT asynchronous interconnection has many different parameters, operating situations, protection and control functions that are not possible to cover in this study due to time and resource constraints. Therefore, the study's scope is limited to make it reasonably doable. On the other hand, some assumptions are taken to make the analysis closer to real-life concerns. The main study assumptions are as the following:

- The VFT rotor torque computing is based on the required power transfer order and the grids' frequencies in the rotor torque unit and applied directly on the VFT rotary transformer. The DC motor drive and its related control loop are excluded.

- The VFT system is not utilised by all suggested protection and control functions related to examining scenario conditions, such as tie-in busses voltage regulator, multi-stage reactive power compensator, and hierarchical control strategy.

- The frequency response and power reserve contribution study excluded any other power generation plant. It only investigates if the VFT system combined with an ESB response such as a synchronous power plant.

- The interconnected grids are not stiff, and their voltages swang with different power flow conditions.

The 4.1.4 clarifies some more simplifications due to reducing simulation time more detailed.

1.6 Report Structure

The report included the study introduction, the VFT system conceptual and theoretical studies, frequency control theories and the VFT system possible ancillary service, the VFT interconnection test system development and verification, the VFT reactive power flow behaviour and maxim possible active power transfer in different operating scenarios discussion, the VFT dynamic response to grid's frequency disturbances analysis, the study conclusion and likely future works, the report references and appendices.

Chapter 1 - Introduction
It provides background and motivations for performing the study. It defines the study purpose and determines the project objectives. It describes the study methodology for each part and clarifies the study boundaries and specifications. It depicts the study's report structure.

Chapter 2 - Variable Frequency Transformer
It introduces the VFT's concept, structure and components. It also reviewed the VFT potentials in future power systems. It explains the VFT operating theory, the fundamentals, and the study's relevant control schemes. It provides the analytical study of the VFT power flow.

Chapter 3 - Frequnecy Control It describes power systems' general frequency droop characteristics, dynamic response to frequency disturbances and different frequency control stages. It also analysis the VFT dynamic response to frequency events and investigate the VFT's expected potential in frequency control involvement.
Chapter 4 - Test Model Development and Implementation
It describes the model development procedure, including employed components, parameters ratings, and the interconnection topology. Then tests the model with a defined base scenario and verifies the test system by comparing the reactive power flow characteristic results with a scientific paper and analytical studies.

Chapter 5 - Discussion
It determines the different operating situations and represents the VFT power flow characteristics of these scenarios' interconnected grids operating frequency. It also defines a frequency disturbance event and shows the VFT dynamic response. It analyses and discusses the maximum possible active power transfer capability and the VFT interconnection stability.

Chapter 6 - Conclusion and Future Works
It concludes the results and analyses of the VFT reactive power flow behaviour and frequency response. It also suggests future works for further studies of the VFT interconnection limitation in a wide frequency matching interconnections and investigating frequency ancillary service operating potential.

References
The reference communicates the pieces of literature and technical datasheets cited in the report. Still, some literature is reviewed in the study and helped the knowledge development but not included in the references because not mentioned in the report. The appendices represent the hand calculation sheet for the analytical studies and all different operating scenarios simulation reports.

Chapter 2

Variable Frequency Transformers

This chapter reviews VFT's concept, structures, and potential application in future power systems. It describes VFT operations modes, power flow control, frequency shifting, and their relation with the rotor drive torque and power. Fundamental protection and control functions, related operation control, and their sequences stages are explained. It represents the steady-state circuit analysis of the VFT interconnection for reactive power flow study.

2.1 VFT Concept and Structure

Variable Frequency Transformer (VFT) is a bidirectional power transmission equipment. A VFT can transfer power between two asynchronous networks. A VFT structure is based on asynchronous machines, that one electrical network connect to the VFT's stator, and the other-one connect to VFT's rotor. Power flow magnitude and direction, and frequency synchronising is regulated by the control motor drive which is coupled to the VFT's rotor. In this chapter VFT concept and operation theory is discussed and reviewed to make the require theoretical foundation. In the first section VFT concept is described and its structure is depicted. Later, operation theory, power flow, frequency shifting equations, and different applications are reviewed.

A VFT is fundamentally a continuous phase-shifting transformer which operate at an any desire phase angle. The main application of a VFT is connecting two power systems that are operating at the same frequency and control the power flow between them such as a phase-shifting transformer[22]. The conventional phase-shifting transformers suffer from step-wise operation, being slow to help with connected grids stability, and components short life-time due to repetitive physical actions and contacts. The conventional phase-shifting transformers sometimes are used with power-electronic devices to tackle mentioned short-comes, but still power-electronic devices limitations such as harmonics and resonance, low over-load capability, and low thermal time constant, constraints the operation[23]. A VFT as a phase-shifting transformer overcomes all mentioned draw-backs.

A VFT's structure also help controlling power-flow between two asynchronous power systems. The other alternative method for connecting two power grid with different operating frequency is to use back-to-back high-voltage DC connection. The back-to-back HVDC connection also suffers from noticed limitations for power-electronic devices. The essential difference between this two technologies promoting different useful application circumstances for each. The world's first VFT for connecting two power grids in order to regulate the power transfer in between without frequency fluctuation repercussions, has been successfully started commercial operating in early 2004 between the Hydro-Quebec power grid and New-York power grid[24] Figure 2.2.

2.1.1 VFT Concept

A VFT's core is a three-phase rotary transformer with integrated winding on both rotor and stator.[25] The magnetic coupling through the air gap transfer power between the two separate electrical networks that connect to stator and rotor respectively. A variable-speed drive motor is used to facilitate the frequency matching between asynchronous networks with rotating the rotor in either direction, and to supply regulated torque on the rotor to controlling power flow magnitude and direction between the two power systems. Figure 2.1 shows the conceptual system block diagram of the VFT.

Same as any other AC machine, the real power flow through a VFT is related to the phase angle

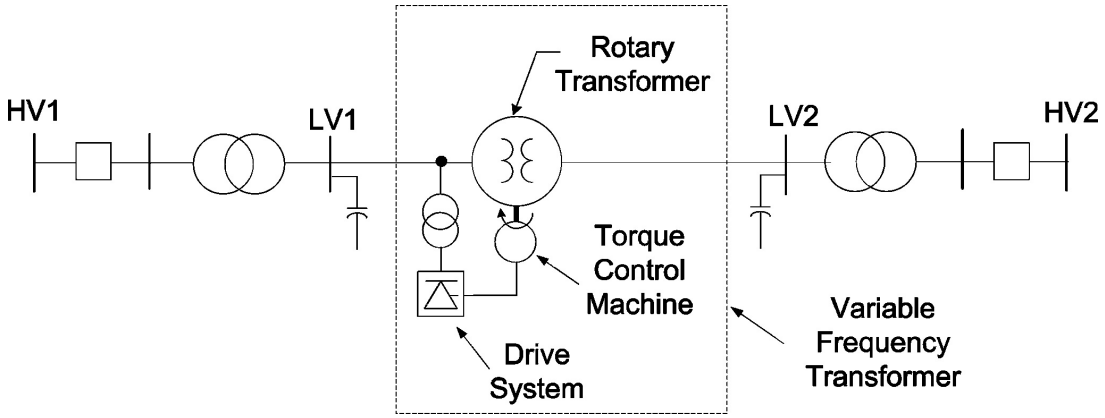

Figure 2.1: VFT conceptual block diagram[22].

difference between stator side and rotor side. For a given power flow the phase angle difference magnitude is determined by considering the impedance of the VFT and two connected grids.

The power flow through a VFT is proportional to magnitude and direction of the applied torque on the rotor by the drive system. In case that two synchronous power systems be connected, the VFT's rotor remains in the position which the stator and rotor voltages are in phase with corresponding systems. If the rotor torque is applied in one direction, then power transfer from the stator side connected network to the rotor side connected network. If the rotor torques is applied in opposite direction, then power transfer also will be inverse from the rotor side connected network to the stator side connected network. The drive system is designed to produce torque continuously while rotor is even standstill. As the power flow is a function of the applied torque on the rotor, then there will be zero power flow through a VFT if no torque apply on the rotor.

In case that two asynchronous power systems be connected, the VFT's rotor rotates continuously with the rotational speed of proportional to the power systems frequency deviation. Load flow also is maintained while drifting frequencies. A VFT is designed to continuously regulate power transfer with frequency matching. Regardless of the power transfer, the rotor naturally orients itself to follow the imposed phase angle difference by the two asynchronous power systems.

A VFT operation is very similar to a back-to-back HVDC converter stations. A VFT has automated energizing, starting, and stopping sequences. In the starting procedure, the VFT nulls the phase angle over the synchronous switch automatically, closes the breaker, and then engages the power regulator controller with zero set point. Then the operator can enter desire set point for the power transfer rate, and the ramp rate value ($power/time$). Power transfer regulation is normal mode of operation. The VFT is equipped with a close-loop power regulator to maintain the power transfer at the level of power rate set-point from the operator. The power rate set-point may be adjusted by other control functions, such as governor, isochronous governor, power-swing damping, and power runback[27].

Power systems are subject to various disturbances, that result in frequency and/or voltage deviations. A VFT's control system constantly involves in maintaining the relative rotor position with respect to the stator, in order to compensate any frequency variation across the two connected power systems. The frequency drifting control loop facilitates constant power transfer. The power regulation control loop is fast enough to take action with power systems events and maintain a stable power transfer. The VFT stations are designed for wide range of system status such as normal, abnormal, and extreme condition, in order to ensure a proper normal operation and sufficient robustness if any network disturbances happen.

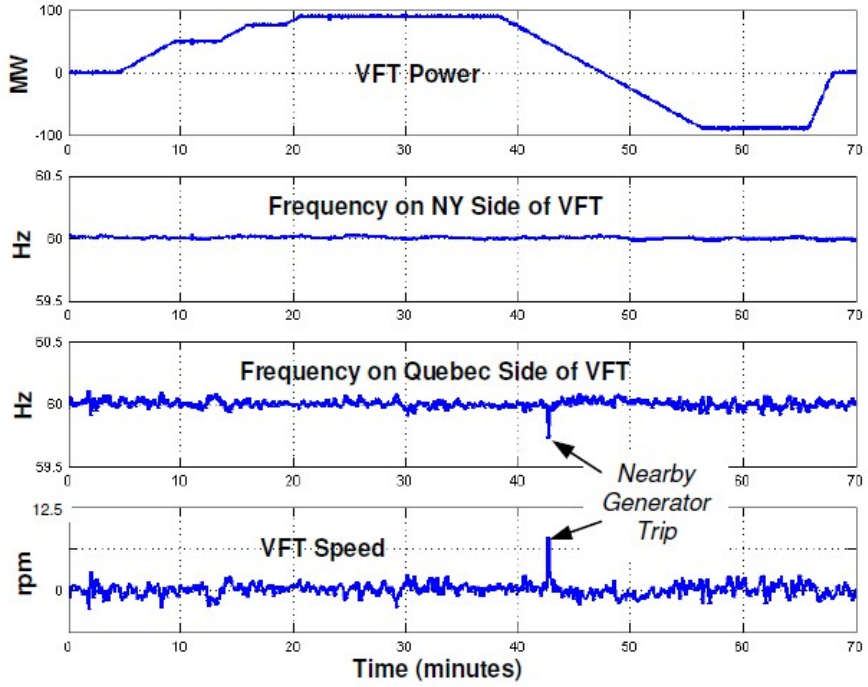

Figure 2.2: VFT power ramps and rotor speed during normal operation between the NY and QC power networks at Langlois substation[22].

Figure 2.2 shows the frequency level in **New York** and **Quebec** networks and a successful recovery from a local disturbance in **Quebec** power system, during an actual operation with variant power transfer rate.

2.1.2 VFT Structure and Components

VFT is composed of three main part, a rotary transformer, a drive motor, and collectors. The rotating structure is the core of system.

Figure 2.3 shows various components of a VFT. The rotary transformer is a conventional wounded

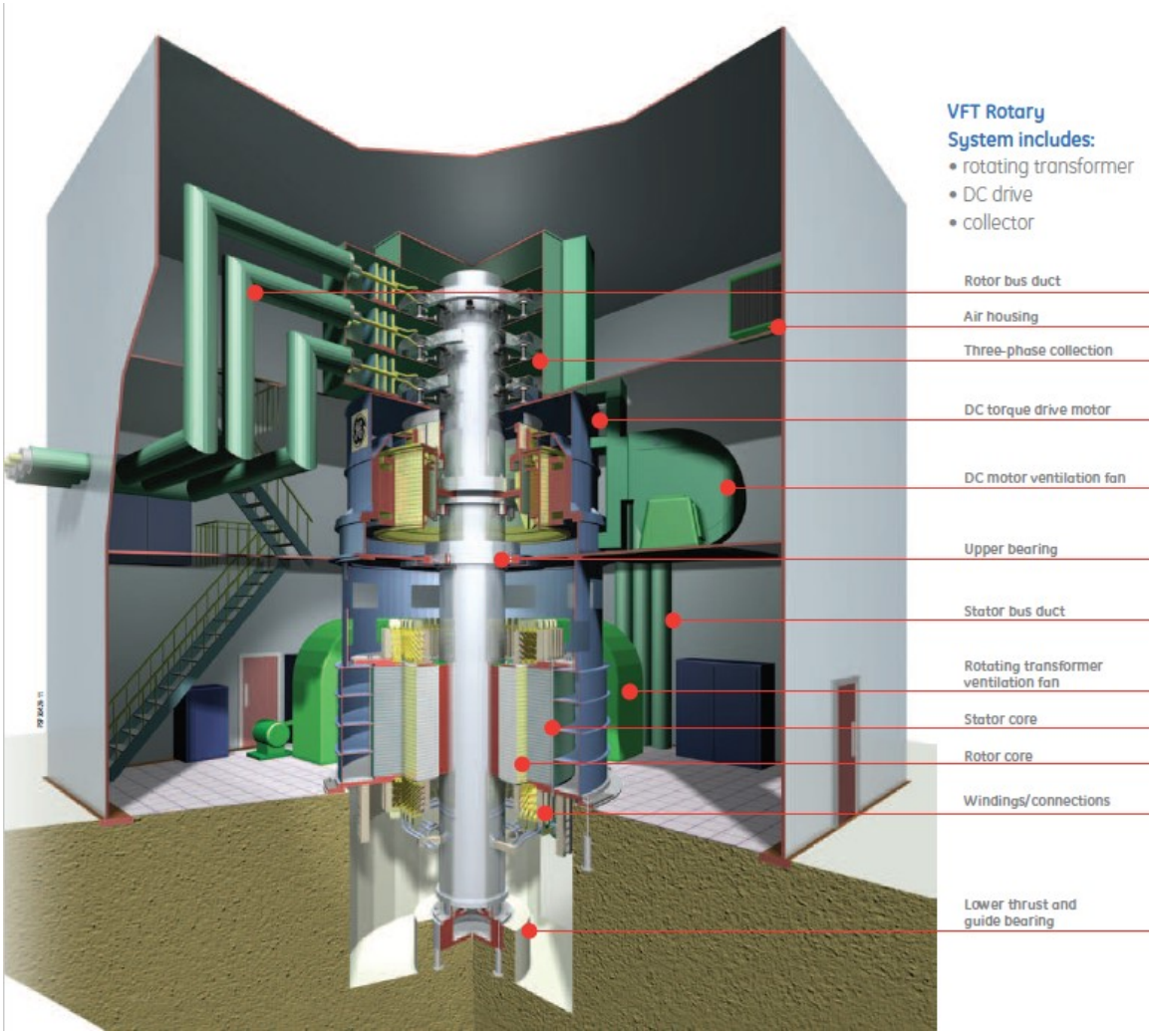

Figure 2.3: VFT components[28].

rotor electrical machine with three-phase winding on both the rotor and the stator. The three isolated phase collector located at top of the rotary system, with conventional technology of carbon brush on copper slip rings. The collector rings are connected to the rotor windings by a three-phase bus. The drive motor is a DC motor that can regulate the torque and rotate in either direction. Considering slow rotational speed of the VFT rotor, a forced air cooling is required. The total rotary system inertia is relatively large. For a 100(MVA), four poles, 60(Hz) the rotating part have an equivalent H-factor of approximately 26(pu-s). This large inertia is the VFT advantage to maintain stability during power network disturbances.

2.1.3 Potential Applications of VFT Asynchronous Interconnection

Merging separated power grids to a super grid with various RES besides the different peak times and seasons in distinct regions, help to overcome the RES fluctuations. Electric power grids interconnection with making power flow between different areas, developing power grids' reliability, and balancing mismatches in supply and demand in an area[11]. The improved power grids' reliability increases power operators' service quality and decreases power interruptions. It also facilitates power sources flexibility and diversity that enhances the energy security besides reducing energy cost as well as power grids development costs[12][13].

Interconnections should be simple, applicable for both synchronous and asynchronous power grids, cost-efficient, secure for power grids, and reliable. High voltage direct current (HVDC), the variable frequency transformer (VFT) and flexible asynchronous alternative current links (FASAL) are available technologies for asynchronous interconnections[19]. Considering FASAL technology is still in the research and development phase, HVDC and VFT are commercialised technologies for comparative analysis.

HVDC

HVDC is an alternative technology to connect two independent power systems through a high voltage direct current (HVDC) system. HVDC systems are developed in varied topologies and technologies such as LCC-HVDC, VSC-HVDC light and MMC-HVDC. According to operating conditions and interconnection location, the HVDC system can have a back-to-back or point-to-point configuration or have monopolar or bipolar DC link. In monopolar-HVDC systems, converters are connected through a single line, and the ground is used for the returning path. Bipolar-HVDC systems use two conductors with positive and negative polarity to connect converters. Monopolar HVDCs are conventionally utilised offshore power transfer to reduce costs. At the same time, bipolar HVDC has the advantage of operating as a monopolar HVDC with the ground link in case of one conductor failure. Valve group firing angle, controls power flow between the connected power systems through the classical HVDC systems [17]. While voltage source converter (VSC) HVDC systems provide full active and reactive power flow control. VSC-HVDCs are conventionally used for long-distant power transfer, where the DC link is utilised as the transmission line[18].

Comparison

Compared to the VFT technology, HVDC systems suffer from complexity, significantly more installation space requirement, high harmonic generating, high impact on nearby generators, complicated integration with grids, no black-start capability, less fault handling due to less thermal capacity and higher control interactions[19][21][26]. Economic evaluation in [20] also confirms a VFT tie-in with the same performance requires around 70% less investment capital compare to an HVDC interconnection. Table 2.1 summarises a comparative analysis between VFT technology and two different HVDC systems.

Table 2.1: Comparison between asynchronous power grids interconnection technologies [19][21][26][20].

	VFT	**LCC-HVDC**	**VSC-HVDC**
Efficiency	High	High	Low
Complexity	Low	High	High
Space requirement	Low	High	Industry standard
Harmonic generating	Very Low	High	High
Impact on adjacent generator	Low	High	High
Grid integration	Easy	Difficult	Industry standard
Black start capability	Yes	No	Industry standard
Bump-less start-up	Yes	No	Yes
Control interaction	Low	High	High
Modular design capability	Yes	No	Yes
Investment Cost	Low	High	High

VFT, as a flexible AC transmission system (FATCS), utilise the power system operating requirement of counteracting electrical disturbances before they impact other parts of the grid and suppressing resonance and low-frequency electromechanical oscillation (LFEO) instability[35]. The inter-area LFEO could inversely impact the power transmission capacity in tie links and threaten the power system's dynamic stability. Increasing the penetration of PV and wind power plants exceeds the LFEO problem that needs to be resolved for renewable energy growth [14]. Employing VFT tie-in at converter base power plants introduces inter-area LFEO damping and improves power system stability. The 2.3 introduce the power-swing damping control function in UVC, which also present an excellent opportunity for the VFT system to facilitate stable and reliable PV and wind power plant integration in power grids. In the same way, VFT facilitates weak power systems connections to main grids. It will eliminate the weak systems' stability and reliability integration risk by repressing the weak grid's disturbances without impacting the main grid[40].

VFT also improves the power quality and efficiency of both new and conventional renewable energy sources. For instance, VFT can overcome offshore wind farms' poor power quality caused by their inherent power fluctuation and increase hydro-power plants efficiency by utilising operating at variable speed[36][37][39].

VFT by supplying reliable, stable and sustainable adjustable power flow promoting optimised

power flow achievement for the grid operators, and helps overcome one of the smart girds' challenges. Plug and play capability of distributed energy sources (DES) causes connecting and disconnecting many DESs at once, which leads to extensive power mismatch and severe frequency and voltage problems[45]. VFT by providing flexible power flow direction and magnitude repress the power mismatch. VFT also provides a resynchronisation function during DESs transition from island to grid mode that facilitates PMS/EMS in smart grids[46].

2.2 VFT Operation Theory

This section describes key but simplified relations for understanding a VFT operating theory. Here only addressed active power transfer and frequency relations, with neglecting the leakage and magnetizing inductance[22]. Represented equations and theory in this section are not sufficient for reactive power study of a VFT but necessary for modelling procedure and forming a concrete theoretical foundation to expand later in section 2.4.

2.2.1 Power Flow

The applied torque on a VFT's rotor regulates the power transfer through the VFT. Can approximate the power transfer magnitude by[30]:

$$P_{VFT} = \frac{V_{L1}V_{L2}}{X_{VFT}} sin(\theta_{L1} - (\theta_{L2} + \theta_{rm})) \tag{2.1}$$

Where P_{VFT} is the transfer power through the VFT from stator to rotor, V_{L1} is the grid#1 side low-voltage buss at stator terminal voltage magnitude, V_{L2} is the grid#2 side low-voltage buss at rotor terminal voltage magnitude, X_{VFT} is the total reactance between the VFT's stator and rotor terminals, θ_{L1} is the voltage angle of the grid#1 side low-voltage buss at stator terminal respect to the reference phasor, θ_{L2} is the voltage angle of the grid#2 side low-voltage buss at rotor terminal respect to the reference phasor, and θ_{rm} is the VFT's rotor phase-angle respect to the VFT's stator. Considering the phasor relationship as shown in Figure 2.4 that V_s represents the V_{L1}, V_r represents the V_{L2}, θs represents θ_{L1}, and θr represents θ_{L2} power. transfer magnitude can be approximated as:

$$P_{VFT} = \frac{V_{L1}V_{L2}}{X_{VFT}} sin(\theta_{net}) \tag{2.2}$$

The Equation 2.2 shows that the theoretical maximum power transfer through a VFT occurs when the θ_{net} is equal to $\pm 90°$. The absolute value for the possible maximum power transfer

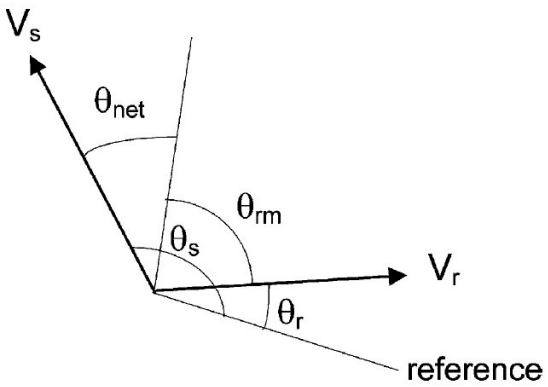

Figure 2.4: VFT phasor relationship (not scaled)[31].

through a VFT is given by:

$$P_{MAX} = \frac{V_{L1}V_{L2}}{X_{VFT}} \tag{2.3}$$

With the stability concerns, the net angle (θ_{net}) must have an absolute value less than 90°. It suggest that the power transfer will be equal to some friction of the theoretical maximum possible power transfer given by Equation 2.3. The power transfer rate can be linearized around the maximum value by:

$$P_{VFT} \cong P_{MAX}\theta_{net} \tag{2.4}$$

Where the net angle (θ_{net}) value is in radians.

2.2.2 Frequency Shifting

Since a wounded rotor induction machine behaves as a transformer at a standstill, ampere-turns must balance between stator and rotor:

$$N_s I_{g1} = -N_r I_{g2} \tag{2.5}$$

Where N_s is the machine stator's windings number of turns, N_r is the machine rotor's windings number of turns, I_{g1} is the current from grid#1 goes through the machine stator's windings, and I_r is the current from grid#2 goes through the machine rotor's windings. Although the coupled power systems are asynchronous, both stator and rotor windings link the same magnetic flux. Hence the voltages also differ by the same ratio. Stator and rotor's voltages can be expressed as:

$$V_{L1} = N_s f_{g1} \Psi_a \tag{2.6}$$

and

$$V_{L2} = N_r f_{g2} \Psi_a \tag{2.7}$$

Where V_{L1} and V_{L2} are the same from Equation 2.1, f_{g1} is the grid#1 electrical frequency on the stator's windings, f_{g2} is the grid#2 electrical frequency on the rotor's windings, and Ψ_a is the air-gap magnetic flux. Considering the induction machine nature, the rotor speed in steady-state is proportional to the electrical frequency deviation between the rotor and stator's windings, which can be shown as:

$$f_{rm} = f_{g1} - f_{g2} \tag{2.8}$$

Where:

$$\omega_{rm} = f_{rm} \frac{120}{N_p} \tag{2.9}$$

Where f_{rm} is the machine's rotor mechanical speed in the electrical-frequency unit, ω_{rm} is the machine's rotor mechanical speed in revolutions per minute, and N_p is the machine number of poles.

2.2.3 Rotor Drive Torque and Power

Figure 1.1 illustrates power flow through a VFT system between two connected power grids and the VFT's rotor control drive. However, the actual power flow direction could be positive or negative depending on the operating condition. Power balance demands that all the power flow into an ideal induction machine combine to zero:

$$P_{g1} + P_{g2} + P_D = 0 \tag{2.10}$$

Where P_{g1} is the active power from the grid#1 into the VFT's stator, P_{g2} is the active power from the grid#2 into the VFT's rotor, and P_D is the VFT's rotor control drive required power that obtains from the connected grid. Equation 2.10 could be written as:

$$-P_D = P_{g1} + P_{g2} \tag{2.11}$$

Assuming the power factor at both side of the machine equal at unity, from the Equation 2.5 and Equation 2.7 we can expand more as:

$$-P_D = V_{L1} I_{g1} + V_{L2} I_{g2} = V_{L1} I_{g1} - (N_r \frac{V_{L1}}{N_s} \frac{f_{g2}}{f_{g1}})(N_s \frac{I_{g1}}{N_r}) = V_{L1} I_{g1} (1 - \frac{f_{g2}}{f_{g1}}) \tag{2.12}$$

or,

$$-P_D = P_{g1}(1 - \frac{f_{g2}}{f_{g1}}) \tag{2.13}$$

As shown in Equation 2.13, the required power in synchronous power systems connection is zero, considering no rotor rotation. The required produced torque by the VFT's rotor control drive can be expressed as:

$$T_{rm} = \frac{P_D}{f_{rm}} \tag{2.14}$$

Using Equation 2.6 and Equation 2.13 to expand more as:

$$T_{rm} = V_{L1} I_{g1} \frac{(f_{g1} - f_{g2})/f_{g1}}{f_{g1} - f_{g2}} = V_{L1} \frac{I_{g1}}{f_{g1}} = N_s f_{g1} \Psi_a \frac{I_{g1}}{f_{g1}} \tag{2.15}$$

or,

$$T_{rm} = N_s I_{g1} \Psi_a \tag{2.16}$$

From Equation 2.16 can be noted that the produced rotor torque is independent of the rotor's rotational speed, and it is only proportional to the current from the grid#1 through the stator's windings and the air-gap magnetic flux. Since the air-gap magnetic flux is nearly constant during the machine operation, the produced torque is only proportional to the current from the grid#1 through the stator's windings. Consequently, with a fixed frequency on the stator-side power grid, the applied torque by the rotor control drive is proportional to the power flow through the VFT. Also, the power transfer in either direction is related to the applied torque on the rotor.

2.2.4 Reactive Power

Figure 1.1 shows the reactive power flow from both connected power grids. The magnitude of each power grid reactive power injection depends on the operating condition. It can be expressed as:

$$Q_{g1} + Q_{g2} = Q_{VFT} \tag{2.17}$$

Where Q_{g1} is the reactive power flow from the grid#1 into the VFT's stator windings, Q_{g2} is the reactive power flow from the grid#2 into the VFT's rotor windings, and Q_{VFT} is the VFT's total reactive power consumption. A VFT's total reactive power consumption can be separated to the reactive power consumed by the magnetizing reactance Q_m and the combined reactive power

consumed by the VFT's stator and rotor leakage reactance Q_l.

2.3 VFT Control and Protection

Proposed protection and control functions in different pieces of literature are based on various applications. This study explains the fundamental protection and control unit that utilised the Langlois VFT substation and the proposed hierarchical control scheme related to the study's primary aim, VFT asynchronous interconnection.

2.3.1 Fundamental Control and Protection

In the first commercial installation of VFT in Langlois substation, digital processors arranged in a modular configuration for each VFT. A VFT unit is controlled by the unit VFT control(UVC) system, that included automated sequencing functions, power transfer regulator, governor, reactive power control, power runback and different monitoring functions. The used control functions are described in the following[26].

A. Governor

The governor control function assists in case the connected power system's frequency exceeds a dead-band threshold during a major disturbance. It will regulate the power transfer rate to adjust the grid frequency to the normal range. The VFT is designed to operate with one isolated side. The VFT intended to operate in the islanded situation connected to the hydropower plant. It supports the required power demand from the isolated grid or reduces the power flow to prevent surplus power mismatch and share frequency control with the local power generator. The VFT isochronous governor helps regulate the isolated network frequency back to the nominal frequency, 60(Hz), with operator engagement.

B. Power-Swing Damping

This control function adds damping to inter-area low-frequency electromechanical oscillations (LFEO) in the range of 0.2(Hz) to 1(Hz).

C. Power Runback

This control function assists to quickly recovering the power level to the preset value. Major network events such as the loss of a generator or critical line loss externally trigger this control function. It prevents power mismatch in the network. The present power order is -65(MW) in the Langlois substation to avoid transmission overloading in case of link loss and power rejection from other grids.

D. Reactive Power Compensation

The VFT like any other transformer has leakage reactance that consumes reactive power related to passing current through it. In Langlois substation shunt capacitor banks are installed, and are switched on/off to compensate the reactive power consumption of the VFT and transmission network. This control function works in three modes, *Power Schedule Mode* that works as a function of VFT power transfer rate, *Voltage Mode* that switches capacitor banks to maintain the bus voltage within the stable range, and *Manual Mode* that operator switches the capacitor banks on/off.

In Langlois substation a VFT is protected by redundant protection system unit. The protective functions are typical protection system for generating plants/AC substations, including ground fault, differential, negative sequence, over-voltage, over-current, over-excitation, breaker failure, capacitor protection, and synchronization check.

The UVC and protection units are essentially identical for each VFT unit. All data from UVC processors, digital relays, and other intelligent electronic devices are gathered to the main VFT control (MVC) system. The MVC also contains higher level control functions for the entire VFT station. It also facilitate the SCADA to enable unmanned operation. The MVC's main purposes are to support the operator interface, SCADA interface, and to coordinate a multi VFT unit.

2.3.2 Asynchronous Interconnection Establishing Control

[38] proposed a practical establishing control approach for two asynchronous power systems interconnection through a VFT. This section describes this 3-stage control strategy. The hierarchical control scheme is upon the asynchronous tie-in configuration depicted in Figure 2.5. The VFT stator is connected to the power network 1 with a frequency equal to f_{PN-I} and phase angle equal to θ_{PN-I}. The power network 2 with a frequency of f_{PN-II} and phase angle of θ_{PN-II} is connected to the VFT rotor.

Stage-1, Frequency Matching

The asynchronous interconnection is initiated by closing the CB1. Induced voltage on the VFT rotor's frequency, f_r, is measured. With an idle rotor, it is supposed to be equal to f_{PN-I}. In order to have the desired frequency matching, the DC motor drive should revolve the rotor to change f_r from f_{PN-I} to f_{PN-II}. The VFT rotor mechanical speed for desired frequency matching in revolutions per minute based on Equation 2.9 is:

$$N_{ref} = \frac{120(f_{PN-I} - f_{PN-II})}{P} \tag{2.18}$$

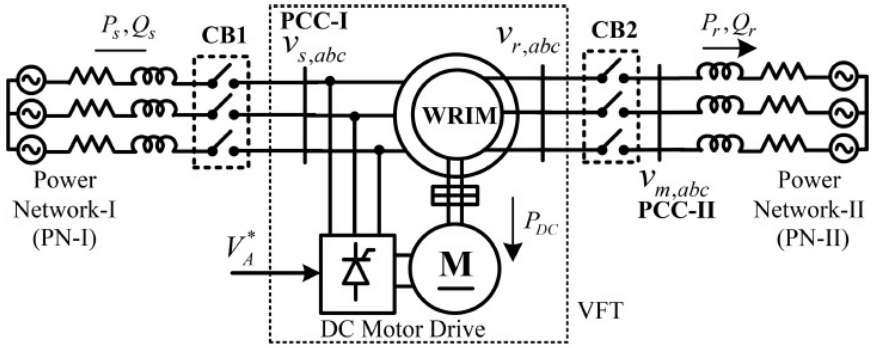

Figure 2.5: VFT system configuration for asynchronous interconnection [38].

Where P is the VFT number of poles. The VFT rotor actual speed N_{act} is measured and compared against the N_{ref} and generates VFT rotor speed error. The frequency matching stage continues until this error gets below the acceptable tolerance.

Stage-2, Phase Angle Matching

The CB2 is still open in this stage, and only CB1 is closed. In this stage, θ_{PN-II} is obtained by the phase locked loop (PLL). Applying abc-dq transformation on the VFT rotor induced voltage using obtained θ_{PN-II}, gives the direct and quadrature components of the VFT rotor voltage, V_{rd} and V_{rq} respectively, referred to the PN-II voltage phasor. When the VFT rotor voltage phase angle, θ_r, and θ_{PN-II} matched, V_{rq} becomes zero. The VFT rotor angle is adjusted until obtained V_{rq} becomes zero or less than the acceptable tolerance.

Stage-3, Power Transfer Control

Now the CB2 closes to establish two power networks interconnection. Reference power transfer order and measured actual transfer power compared to compute the required rotor torque by the DC motor drive. In this stage, any power networks frequency changes force the rotor speed adjustment according to the Equation 2.18.

2.4 Analytical Study

The previously expressed equations for power transfer through a VFT are insufficient for the VFT reactive power flow analysis as they neglect leakage and magnetising inductance of the WRIM[29]. These inductances are significant for a 100(MW) induction machine and primary source of the reactive power requirement of the VFT operating. In this matter, to study the reactive power flow behaviour of a VFT in an asynchronous interconnection analytical study to take

part in the leakage and magnetising inductances.

2.4.1 VFT Power Flow

As explained in 2.1.2, the rotary transformer of a VFT is essentially a wound rotor induction machine (WRIM). The analytical study of the VFT power flow conducts over the WRIM equivalent circuit. Figure 2.6 shows the steady-state equivalent circuit of a WRIM as referred to the stator-side.

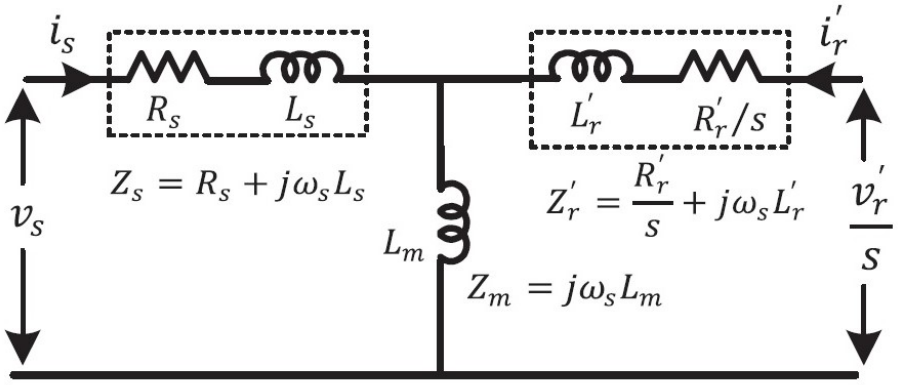

Figure 2.6: WRIM steady-state equivalent circuit[29].

Where v, i, R, L, Z, and S represents voltage, current, resistance, inductance, impedance and slip respectively. While subscripts s and r refer to the stator and rotor side values, superscript $'$ shows the rotor-side values referred to the stator-side. According to the analysis offered in the appendix A, the VFT instantaneous stator current can be expressed by:

$$i_s = v_s\left(\frac{Z_m + Z_r'}{Z_m Z_s + Z_m Z_r' + Z_s Z_r'}\right) - \frac{v_r'}{S}\left(\frac{Z_m}{Z_m Z_s + Z_m Z_r' + Z_s Z_r'}\right) \tag{2.19}$$

And the instantaneous rotor current referred to the stator side can be written as:

$$i_r' = \frac{v_r'}{S}\left(\frac{Z_m + Z_s}{Z_m Z_s + Z_m Z_r' + Z_s Z_r'}\right) - v_s\left(\frac{Z_m}{Z_m Z_s + Z_m Z_r' + Z_s Z_r'}\right) \tag{2.20}$$

Applying superposition theorem also gives the same result. The active and reactive power flow from Grid#1 and Grid#2 is given by:

$$P_{g1} = real(v_s i_s^*) \tag{2.21}$$

$$Q_{g1} = imag(v_s i_s^*) \tag{2.22}$$

$$P_{g2} = real(v_r i_r^*) \tag{2.23}$$

$$Q_{g2} = imag(v_r i_r^*) \tag{2.24}$$

Equation 2.17 gives the total reactive power requirement for the VFT operation equal to:

$$Q_{VFT} = Q_{g1} + Q_{g2} \tag{2.25}$$

2.4.2 Power Networks tie-in Equivalent Circuit

Considering that the grids' voltage and tie-in impedances affect the VFT stator and rotor voltage, an equivalent circuit for the tie is also essential for further power flow analytical study. Figure 2.7 and Figure 2.8 shows the grids' tie-in to the VFT stator and rotor configuration.

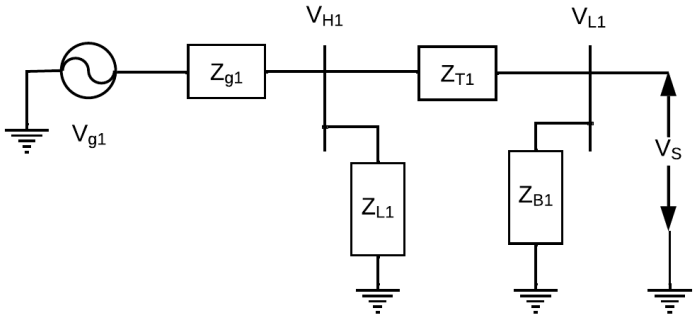

Figure 2.7: Grid1 Tie-in to the VFT stator single-line diagram.

Thevenin's theorem obtains the equivalent tie-in circuit. In the appendix A detailed analysis for getting thevenin equivalent voltages and impedances are shown. Equivalent thevenin voltage source the VFT stator terminals seen is:

$$V_{S,Th} = V_{g1} \frac{Z_{T1}Z_{L1} + Z_{B1}Z_{L1}}{Z_{T1}Z_{L1} + Z_{B1}Z_{L1} + Z_{g1}Z_{T1} + Z_{g1}Z_{B1} + Z_{g1}Z_{L1}} \frac{Z_{B1}}{Z_{T1} + Z_{B1}} \tag{2.26}$$

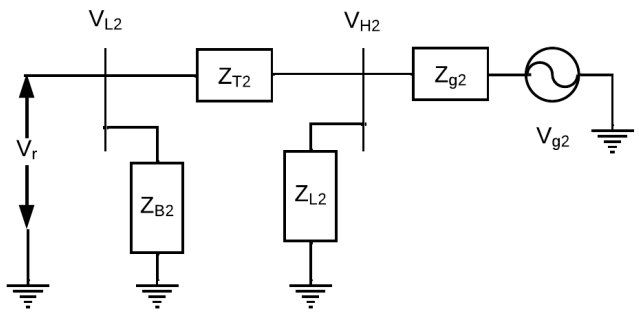

Figure 2.8: Grid2 Tie-in to the VFT rotor single-line diagram.

And equivalent thevenin voltage source the VFT rotor terminals seen is:

$$V_{R,Th} = V_{g2}\frac{(Z_{B2} + Z_{T2})||Z_{L2}}{((Z_{B2} + Z_{T2})||Z_{L2}) + Z_{g2}}\frac{Z_{B2}}{Z_{B2} + Z_{T2}} \tag{2.27}$$

The VFT stator side tie-in thevenin equivalent impedance is:

$$Z_{S,Th} = \frac{Z_{g1}Z_{L1}Z_{B1} + Z_{g1}Z_{T1}Z_{B1} + Z_{L1}Z_{T1}Z_{B1}}{Z_{g1}Z_{L1} + Z_{g1}Z_{T1} + Z_{L1}Z_{T1} + Z_{g1}Z_{B1} + Z_{L1}Z_{B1}} \tag{2.28}$$

And the VFT rotor side tie-in thevenin equivalent impedance is:

$$Z_{R,Th} = ((Z_{g2}||Z_{L2}) + Z_{T2})||Z_{B2} \tag{2.29}$$

Chapter 3

Frequency Control

This chapter describes the frequency control in power systems. It clarifies power systems' general frequency droop characteristics and defines the primary and secondary frequency control related to the study's objectives. It represents the frequency response dynamic stages in a synchronous power plant and analyses how the VFT system can implement for frequency response improvement. It reviews the Norwegian grid code for integrating wind farms into the power grid.

3.1 Power System Frequency Control

Figure 3.1 shows the power system response and different frequency control levels for recovering the frequency drop because of severe power mismatches. Transmission power links loss or power plant tripping can be the reason for a large frequency disturbance. This study focuses on inertial, primary and secondary frequency control, stage II, III, and IV, considering the VFT system's structure. Although the WRIM in the VFT system contribute to the rotor swing naturally, and the VFT power-swing damping control function improves the system stability, the dynamic analysis of the VFT rotor swing is not the focus of this study.

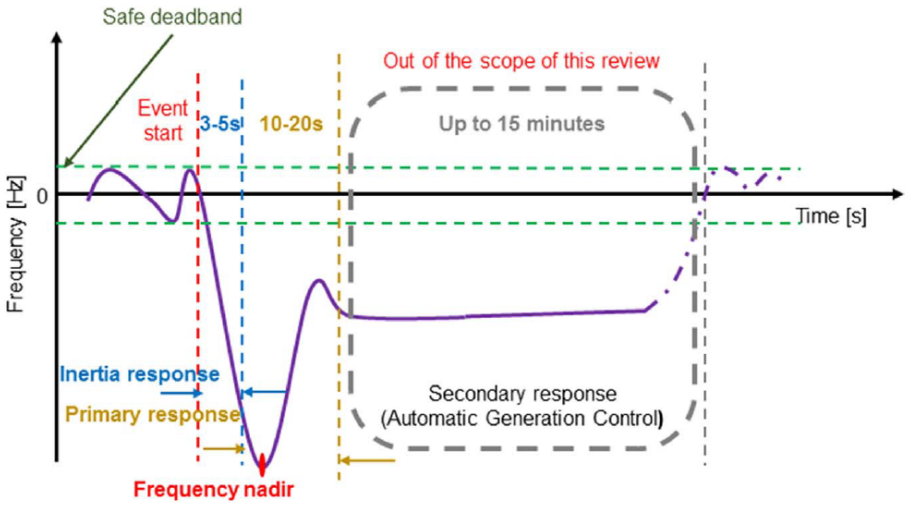

Figure 3.1: Power plant response to mitigate the frequency drops[50].(Secondary frequency control is considered in this study))

The inertial frequency control, stage I, is the natural response of the conventional power plants, and no control system contributes to this stage. It acts inherently just after the frequency disturbance because of power mismatch but does not take long. Nevertheless, new studies introduce the synthetic inertia in the DFIG control loop and study its impact on system frequency response improvement [47]. The primary frequency control is the local level control by the power plants to deliver their reserved power capacity. Different power reserve control approaches are taken in wind farms to have a safe and efficient integration in the power market. The 20% marginal power reserve is the most common power reserve strategy, which power operators also request for safety reasons. The secondary frequency control is centralised to recover the remained frequency deviation back to normal. Central automatic generating control based on different factors communicate with power plants for frequency ancillary service through the supervisory control system.

3.1.1 Stage II - Frequency Drop

In conventional power plants, synchronous generators convert the rotational mechanical energy from turbines to electrical power. These turbines are utilised with a governing system that controls the turbine rotational speed at the desired rate considering the electrical grid operating frequency and the coupled generator number of poles. In any electrical power demand change from the grid, the governor regulates the rotational speed to set back the generator power frequency on the reference value. In increasing, power demand events, such as another power plant tripping before the turbine governor act, the rotational kinetic energy stored in the turbine compensates for the energy loss in the system. This phenomenon is known as power plants inertia. The power sources are connected to the power grid through power electronic converters in RES technologies, except for the hydro plants equipped with turbines and synchronous generators. Recently with growing the asynchronous wind turbines technology, even wind turbines that have stored kinetic energy do not contribute to the inertial response to frequency disturbances. However, recent studies introduced synthetic inertia to improve this deficiency of wind turbines [49].

For studying the inertial response of the power generating system, start from the swing equation from [30]:

$$J\frac{d\omega}{dt} = \tau_m - \tau_e \tag{3.1}$$

Where J is the turbine moment of inertia, ω is the rotation speed, τ_m is the mechanical torque applied from the turbine, and τ_e is the electrical torque on the rotor. Substituting the J with the inertial time constant, H gives:

$$\frac{d\omega}{dt} = \frac{\omega_s^2}{2HS_n}\Delta\tau \tag{3.2}$$

Where ω_s is the synchronous speed, and S_n is the system rated power. Converting to per unit and rewriting the torque in power and rotation speed in synchronous generators with frequency gives:

$$\frac{df}{dt} = \frac{f_0}{2H}\frac{\Delta P}{S_n} = RoCoF \tag{3.3}$$

Where ΔP is the demand power change, and f_0 is the grid nominal frequency. The rate of change of frequency (RoCoF) is an essential factor in the power systems' stability because thermal turbines and many loads may face a critical situation with high RoCoF.

From a comprehensive point of view, the whole power grid's frequency droop characteristic is given by:

$$\frac{df}{dt} = \frac{f_0\Delta p}{\sum 2H_iS_{n,i}} \tag{3.4}$$

Where $S_{n,i}$ is each operating power plant rated power, and H_i is the power plant inertia-time

constant. It shows that higher inertia-time constant and higher rated power result in a higher contribution to the inertial frequency response of the system.

Figure 3.1 shows the power plant response to frequency drops and different levels of a frequency control for recovery of the disturbance. Although the inertial response is part of the primary frequency control, it is part of the natural dynamic response. No controller in conventional power plants contributes to it. However, the new concept of synthetic inertia from wind turbine controllers acts at this level. But this study focuses on synchronous power generators' frequency control.

3.1.2 Stage III - Primary Control

Each power plant turbine governor independently acts and regulates the mechanical power to recover speed loss in this stage if the frequency change is bigger than the defined acceptable dead-band. Based on the droop coefficient of each turbine, the power plant recovers part of the mismatch.

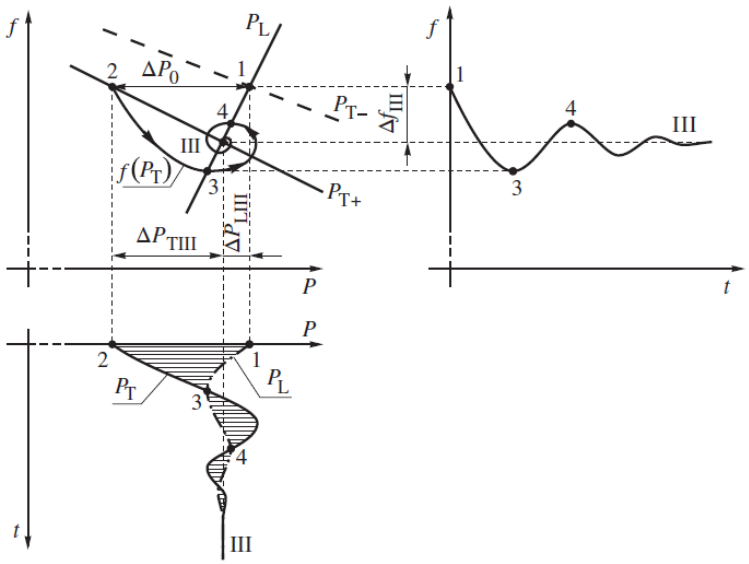

Figure 3.2: Power System Frequency Response Stage III - Primary Control[30].

Like the synchronous power plants' turbine, electrical loads' power demand also changes with frequency. But the loads' frequency sensitivity coefficient is the power plant's opposite sign, which means their power demand decreases with frequency drop. Any power generation loss or sudden power demand rise lead the system to the new power-frequency equilibrium point. Figure 3.2 shows the power generation plants and loads dynamic interaction response that leads to the new operating point. The crucial issue for the power system is to have sufficient spinning

reserve to contribute in this stage.

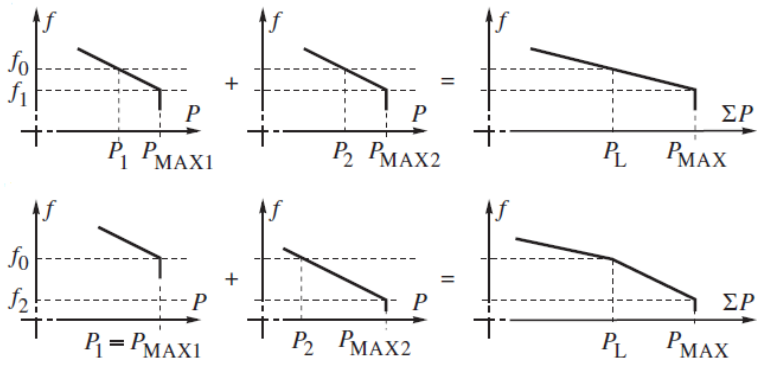

Figure 3.3: Spinning reserve impact on primary frequency control[30].

Figure 3.3 shows how insufficient power reserve for delivering to the system negatively result in more frequency drop and lower frequency nadir.

3.1.3 Stage IV - Secondary Control

At this stage, the central controller adjusts the power reference for each power plant base on the grid's optimal power flow, plant location, power generation limits, and transmission lines' load to prevent any further undesired over-load or disturbances. Power plants turbine governor adopt their power delivery with the new power reference and the grid nominal frequency by shifting the frequency droop characteristic, as shown in Figure 3.4.

3.2 Combined ESB and VFT System as Synchronous Power Generator for Frequency Ancillary Services

This section describes how the VFT system combined with an ESB could be considered a synchronous power generator plant. In synchronous power plants, the mechanical turbine is the source of energy that converts the energy to kinetic energy and apply as the power to the generator shaft. The synchronous generator with the rotor's not rotating magnetic field flux induces a rotating voltage at the generator stator winding. This induced voltage frequency depends on the generator's rotor rotational speed and the machine's number of poles. Considering the described VFT structure and components in the 2.1, and its operating theory 2.2, it works as a transformer at a standstill. Using an ESB on one side of the VFT system to deliver an AC power at the gird

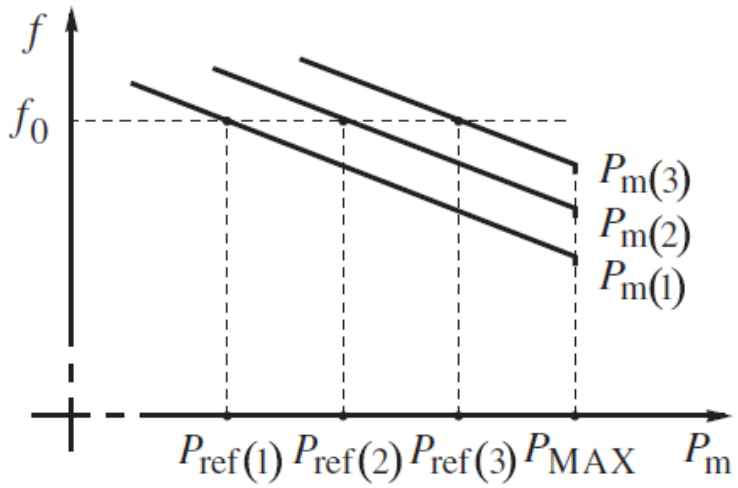

Figure 3.4: Power Plant Frequency Droop Characteristic For Different Power Reference[30].

nominal frequency, the other side would also experience the AC power at the rated frequency. Changing the grid power demand from the VFT system will change the electrical torque, and in the case of a free rotor with no applied torque, it will start to rotate or speed change in synchronous generators. Using the VFT power flow equation, 2.16 the rising power demand from the grid can be provided by the ESB by raising the applied torque on the rotor from the DC motor drive. In VFT systems, the DC motor drive acts as the turbine in the synchronous generating power plants. The low speed droop of the DC motors with raising the torque would also enhance the general power system frequency droop. The bidirectional power transfer by the VFT support charging the ESB in surplus power and over the frequency situation. That also prevents the sensible power plants from operating close to their lower limits.

The VFT system's high inertia constant, 25(pu-s) for the 100(MW) VFT at the Langlois, introduces a natural and reasonable inertial frequency control that could reduce the power system RoCoF. DC motor drive acting time and torque control have been explored in the electrical machines industry for many years and are well-known technology. They provide an adequate primary frequency control by rotor torque and speed control. And their capacity to produce different torque at the same rotational speed with voltage control supports the speed droop characteristic shifting and secondary frequency control.

3.3 Norwegian Grid Code For Wind Farm Integration

With growing RES penetration in power systems, new grid codes and restrictions apply for ancillary services for the power system's safety and reliable distribution. This study investigates the primary Norwegian power grid operator, Statnett, grid code for wind farms integration. Ac-

cording to the study objective, frequency regulations are considered to examine later with the VFT test system response.

Table 3.1: Norwegian power grid operator, Statnett, grid code for wind farm with transformer operating limits[51].

Parameters	**Value**	**Operating Time**
Wind farm voltage	0.9 - 1.05 (pu)	Continuous
Wind farm voltage	1.05 - 1.1 (pu)	60 minutes
Frequency	0.95 - 0.98 (pu)	30 minutes
Frequency	0.98 - 1.02 (pu)	Continuous
Frequency	1.02 - 1.03 (pu)	30 minutes

Table 3.2: Norwegian power grid operator, Statnett, grid code for wind farm frequency control[51].

Parameters	**Value**	**Unite**
RoCoF	0.03	pu/sec
Primary control dead-band	0.01	pu
Frequency droop	2 - 12	%

Table 3.1 represents the wind farm voltage and frequency required operating limit of wid farms. Table 3.2 represents the wind farm's required frequency droop characteristic and the least contribution limits expected.

Chapter 4

Test Model Development and Implementation

This chapter demonstrates the VFT asynchronous interconnection model development procedure in the Matlab/Simulink, defines the topology, describes the used components and their parameters' value implemented in the model. It specifies the simulation setup and model simplifications and their reason and impacts. It shows the base scenario test result and verifies the model by comparing it with analytical calculation results, and a published paper.

4.1 MATLAB\Simulink Model

Matlab\Simulink has been chosen for the modelling and simulation as the Simulink Simscape library provides complete power system components for modelling and simulation of the two grids' interconnection. It is possible to evaluate the power systems' steady-state operation, disturbances responses and power flow at the grid level. It also helps to integrate control systems and test the system performance. Matlab processes the simulations' results, analysis the analytical calculations, compares them and delivers the represented outcomes.

4.1.1 Topology and Components

A comprehensive grids interconnection is modelled to characterise the VFT reactive power behaviour in an asynchronous operation. This study references the world's first VFT interconnection configuration between the Newyork power grid in the US and Hydro-Quebec in Canada in the Langlois substation [24][33]. It has been almost duplicated later in the Laredo substation to utilise power transmission between Texas in the US and Mexico as well [34]. Figure 1.1 illustrates the modelled interconnection single-line diagram based on the Langlois VFT substation topology represented in Figure 2.1.

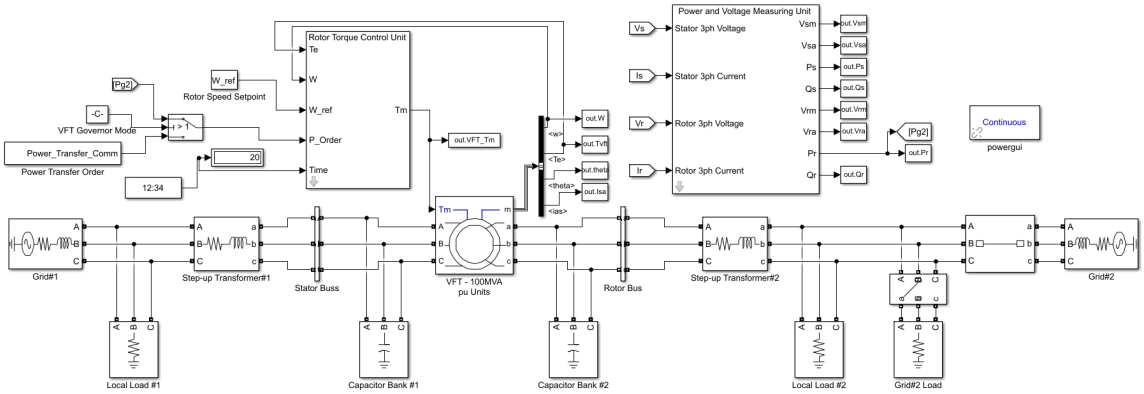

Figure 4.1: VFT interconnection model in Matlab\Simulink.

Figure 4.1 shows the VFT interconnection model developed in Matlab\Simulink. The studied case interconnects two weak power systems with introduced impedances that impact the point of common connection (PCC) of the grids and the VFT tie-in voltage phasor at the high voltage buses. Two purely resistive loads are connected at each high voltage bus to smooth the simulation and represent the VFT interconnection substation local load. These resistive loads are necessary for discrete simulation, and the asynchronous machine module does not work. Still, it smooths the initial transient and reduces the simulation run time and decreases the error range in the continuous simulation mode. Two conventional step-up transformers convert the grids' high voltage to the VFT operating voltage at the low voltage buses. Two series inductances represent

these step-up transformers at each side of the VFT. Two capacitor banks on the VFT stator and rotor side compensate reactive power requirement of the VFT. In the absence of a VFT module in any Simulink libraries, a per-unit wound-rotor asynchronous machine module is employed with direct torque value input from the rotor torque control unit. This WRIM module utilises the sixth order asynchronous machines model. There are four electrical dynamic equations for quadratic and direct voltages on the stator and rotor sides and two mechanical equations for rotor speed and angle. The VFT's rotor torque control unit substitutes the DC motor drive to calculate and applies the required VFT rotor torque based on the reference rotor speed and power transfer order to the VFT rotor. A purely resistive load connects to the grid#2 through a circuit breaker to apply the system power demand increase's event. A circuit breaker utilises disconnecting the $grid\#2$ power source in the severe frequency disturbance.

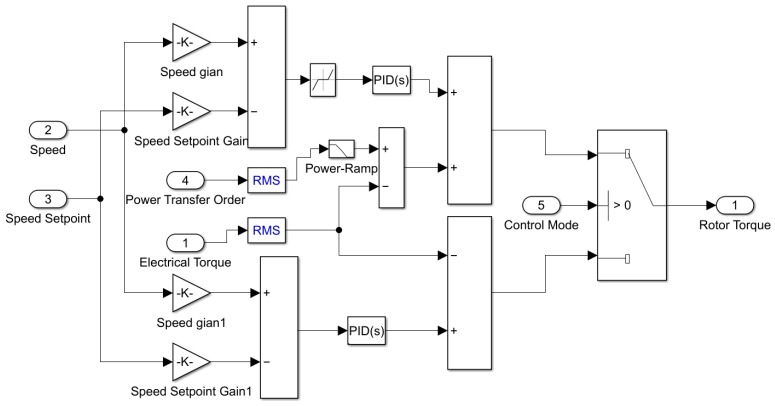

Figure 4.2: VFT rotor drive torque control unit model in Matlab\Simulink.

Figure 4.2 shows the developed rotor torque control unit module in Matlab\Simulink. This module has been designed according to the mechanical dynamic equation of the used WRIM module[43]:

$$\frac{d}{dt}\omega_m = \frac{1}{2H}(T_e - F\omega_m - T_m) \tag{4.1}$$

Where ω_m is the VFT's rotor speed, H is the VFT's inertia constant, T_e is the produced electrical torque in VFT, F is the VFT's friction factor, and T_m is the applied mechanical torque on the VFT's rotor shaft. The rotor torque control unit first only applies the required torque based on frequency matching and then, after the defined time, switches to power transfer and frequency regulating mode. The second torque control mode is utilised with a preliminary PID controller for smoother rotor speed regulation. Still, the controller gains are not optimised in this study, and only roughly acceptable values are introduced. The power transfer order mode also depends on the test mode. It follows a predefined signal for reactive power characteristic studies and follows the grid#2 required power during the frequency disturbance. The dead band zone is also applied to the frequency response.

And the last part in the test model is the power and voltage measuring unit that computes the active and reactive power flow and voltage magnitude and angle based on the measured 3-phase voltage and current at the low voltage buses and the connected grid frequency. Considering this study focuses on the VFT itself reactive power flow behaviour, the power flow is measured at the low voltage buses to ignore the step-up transformer reactive power consumption in any operation situation.

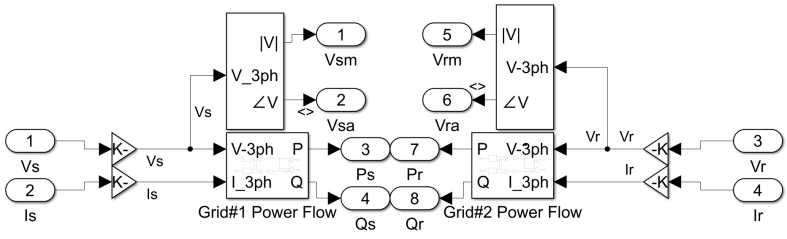

Figure 4.3: Power flow and voltage measuring unit in Matlab\Simulink.

Figure 4.3 shows the power flow, and low-voltage\VFT busses Voltages' magnitude and angles measuring in the Matlab\Simulink in per unit and radian. This module calculates the voltages' phase angle according to each grid base frequency. The voltage phase angle measuring utilises the second stage of hierarchical control strategy for phase angle matching described in 2.3.2. It is also practical for the DC motor drive armature's voltage control loop.

4.1.2 Model Parameters Value

Table 4.1, Table 4.2 and Table 4.3 represent the VFT interconnection parameters obtained from Langlois's installed VFT system [33], including the power, voltage and frequency base values, the WRIM parameters and the reactance of the step-up transformer. Some parameters such as the reactive power compensator capacitor banks and introduced local-load have been modified for smoother simulation and more direct analysis. The capacitor banks values obtained based on the VFT no-load reactive power requirement to null the reactive power flow from the grids at zero active power transfer.

Table 4.1: VFT interconnection base values [33].

Parameters	**Symbol**	**Value**	**Unit**
Nominal Power	S_{Base}	100	MVA
Nominal Line RMS Voltage	V_{Base}	17	kV
Nominal Frequency	f_{Base}	60	Hz

Table 4.2: VFT interconnection WRIM parameters [33].

Parameters	Symbol	Value	Unit
Stator Resistance	R_s	0.001	pu
Stator Reactance	X_s	0.06	pu
Rotor Resistance	R_r	0.001	pu
Rotor Reactance	X_r	0.06	pu
Mutual Reactance	X_m	5.6	pu
Inertia Constant	H	25	pu
Friction Factor	D	0.01	pu
Pole Pairs	P_p	4	
Stator to Rotor Winding Turns Ratio	$n_s : n_r$	1	

Table 4.3: VFT interconnection tie-in parameters [33].

Parameters	Symbol	Value	Unit
Stator Connected Capacitor Bank	B_1	8.8	MVAR
Rotor Connected Capacitor Bank	B_2	8.8	MVAR
Grid #1 Step-up Transformer Reactance	X_{T1}	0.1	pu
Grid #2 Step-up Transformer Reactance	X_{T2}	0.1	pu
Grid#1 Side Local Load	R_1	0.01	pu
Grid#2 Local Load	R_2	0.01	pu

The power grid's impedance or the short circuit ratio (SCR) represent the gird order of stiffness. The gird SCR defines by the ratio between the short circuit power of the grid at the PCC and the grid rated power[41]. [42] suggest SCR of 10 introduces a reasonably weak grid. This study employs girds SCR of 10 with $X/R = 10$. Described grids parameters are represented in Table 4.4.

Table 4.4: Weak grids parameters.(SCR=10, $X/R = 10$)

Parameters	Symbol	Value	Unit
Grid#1 Line-Line RMS Voltage	$V_{LL-RMS1}$	1	pu
Grid#1 Equivalent Resistance	R_{g1}	0.00664	pu
Grid#1 Equivalent Reactance	X_{g1}	0.0664	pu
Grid#2 Line-Line RMS Voltage	$V_{LL-RMS2}$	1	pu
Grid#2 Equivalent Resistance	R_{g2}	0.00664	pu
Grid#2 Equivalent Reactance	X_{g2}	0.0664	pu

4.1.3 Simulation Setup

Different simulation scenarios setts different simulation times according to the power transfer order and frequency deviation. The power ramp time constant is 2 seconds, which means the simulation needs 10 seconds to reach 1(pu) power transfer from zero, giving a smooth power increase to prevent transition mode in the WRIM. Minimum and maximum simulation time steps are determined based on 360 to 3600 signal resolution, with defined 0.1% relative error tolerance for the simulator differential solver. Considering this study focuses mainly on the steady-state behaviour of the VFT and power change events, but not the large disturbances and electromechanical transients, these simulation setup's values help to have enough accuracy in initial transition mode and, at the same time, short run-time.

4.1.4 Model Simplifications

The developed model does not include complete VFT interconnection configuration components, control and protection functions due to the study time limitation and preventing complexity. High voltage buses and voltage and power measuring at those buses are eliminated to reduce the simulation time. The DC motor drive neglected to decrease the model complexity and applied the computed required rotor torque to the WRIM module. The grid sources are fixed voltage and frequency sources, not programmable ones, to reduce the complexity of the model and test scenarios. ESB is also considered a voltage source with a fixed frequency and voltage rate with introduced impedance, but not a complete ESB with power electronic converters. Phase angle matching procedure, the second stage of the hierarchical control strategy explained in the 2.3.2 is also not implemented in the model. So the voltage phase measuring is through Fourier series calculation and not the phase locked loop (PLL) to reduce simulation run time significantly shorter. This simplification results in the VFT frequency service study's voltage measurement error on the grid#2 side. The frequency drop does not reflect at the Fourier series computation window, which is the measurement error source. Multi-stage capacitor banks also substitute with the constant capacitor banks, and they only compensate for the no-load, zero

power transfer order, VFT's reactive power requirement.

4.2 Model Testing

The base scenario tests the developed model for the preliminary evaluation of the VFT interconnection. The main focus of testing is validating rotor torque computation and application by the rotor torque unit and power and voltage measuring while investigating total reactive power consumption of the VFT interconnection and reactive power flow from each grid. Calculating the VFT power factor (PF) in the synchronous operating is also considered.

4.2.1 Base Scenario

This scenario includes two synchronous power grids with the operating frequency of 60(Hz) interconnection. Considering the synchronous interconnection, the rotor torque unit does not perform frequency matching at the beginning of the simulation. Then from 5 seconds to 15 seconds, the power transfer order raise-up to 1(pu) from Grid#1 to Grid#2. Then from 15 seconds to 25 seconds, the power transfer order gets back to zero, and from 25 seconds to 35 seconds, the power transfer order raise-up to 1(pu) from Grid#2 to Grid#1. Each power transfer step takes long enough to fulfil the power ramp requirements of 10 seconds for changing 1(pu).

4.2.2 Preliminary Simulation Results

Figure 4.4 shows the power transfer order and the active power flow from the power grids over time.

Figure 4.5 shows the zero reactive power flow from the grids at the zero power transfer order and their changes with increasing the power transfer order besides the VFT total reactive power consumption over time. The simulation result shows the 19.8(MVAR) reactive power flow at the 100(MW) active power transfer that shows the PF of 0.98 for the 100(MVA) VFT at synchronous full-load operation.

The VFT reactive power flow characteristic upon the power transfer order in the synchronous interconnection is shown in Figure 4.6.

Figure 4.7 shows the apparent power flow through each side of the VFT over time, which slightly violates the VFT rated power 1.94%.

Figure 4.8 shows the voltage magnitude at the low voltage buses both change in the range of $\pm 1\%$ that is ideally acceptable.

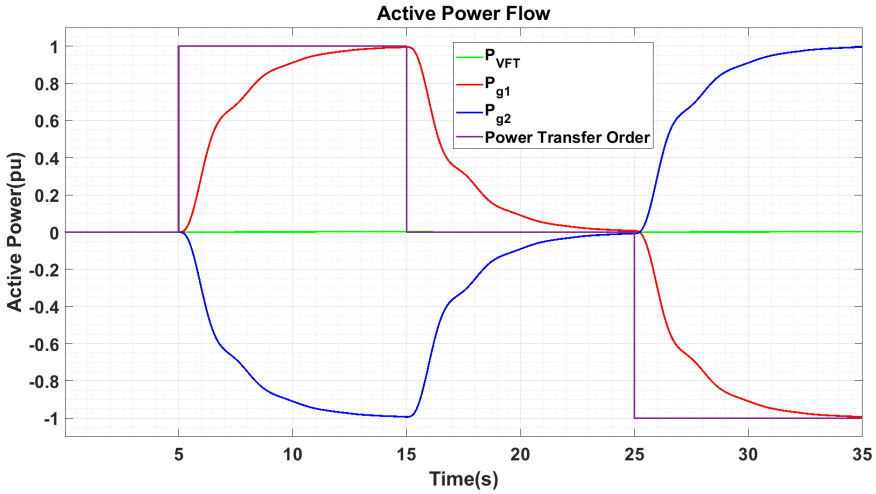

Figure 4.4: Synchronous interconnection active power flow and power transfer order.

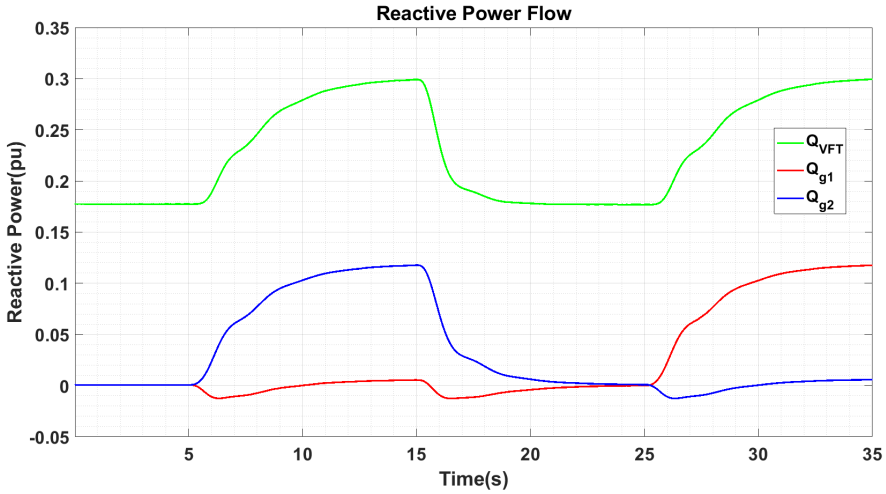

Figure 4.5: Synchronous interconnection reactive power flow.

Figure 4.9 shows the VFT's rotor speed in per unit, that picks in order of $4e^{-}4$(pu) and refers to Equation 2.9, 0.72(RPM) at power transfer order stepping moments at 5, 15 and 25 seconds.

The complete Matlab\Simulink base scenario simulation report is in the appendix B.

4.3 Model Verification

This study verifies the model by comparing the base scenario simulation results with adopted components parameters value, with analytical studies represented in section 2.4 and published

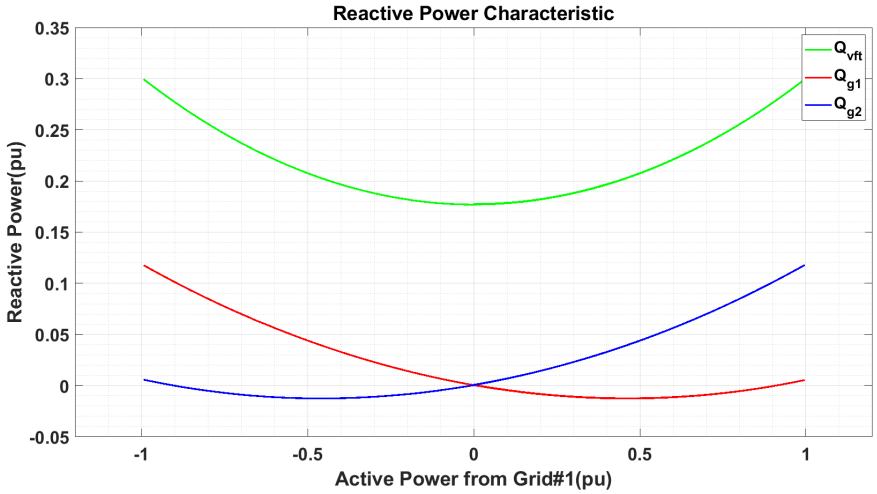

Figure 4.6: Synchronous interconnection reactive power flow characteristic.

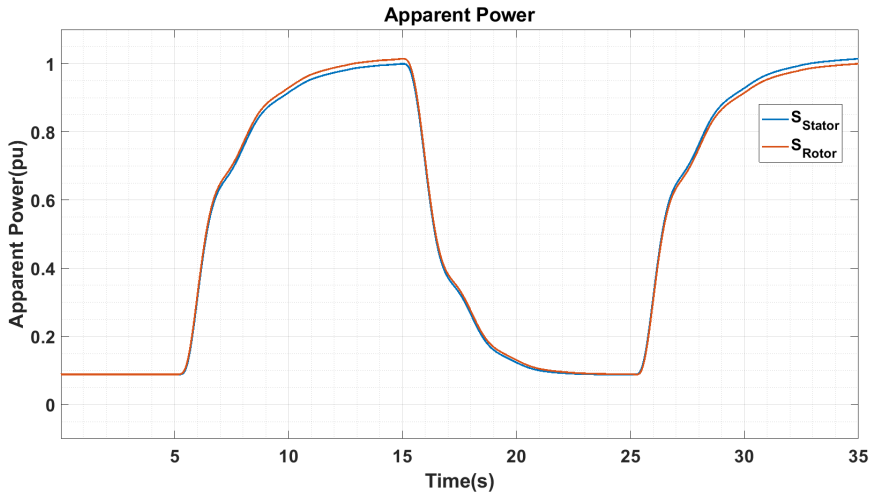

Figure 4.7: Synchronous interconnection apparent power flow through each side of the VFT.

results in research[29]. The model verification scenario is the same as the base scenario defined in the B. The study determines the reactive power flow characteristic based on the active power transfer magnitude and direction with fixed grids' voltage magnitude, and the grid#2 voltage magnitude deviation with fixed active power flow and grid#1 voltage magnitude.

4.3.1 Verification Model Parameters

The verification parameters are distinct from the main model parameters to support comparing and verifying the result with the reference. Implemented parameters according to [29] are shown in Table 4.5,Table 4.6 and Table 4.7. The moment of inertia J in [29] converted to inertia constant H to be compatible with the model, and also some other parameters, including both grids'

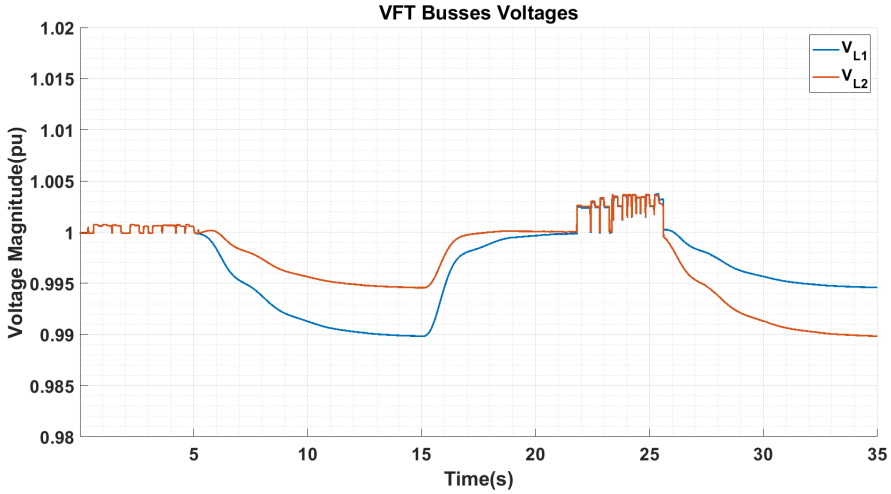

Figure 4.8: The VFT buses voltage magnitude at synchronous interconnection operation.

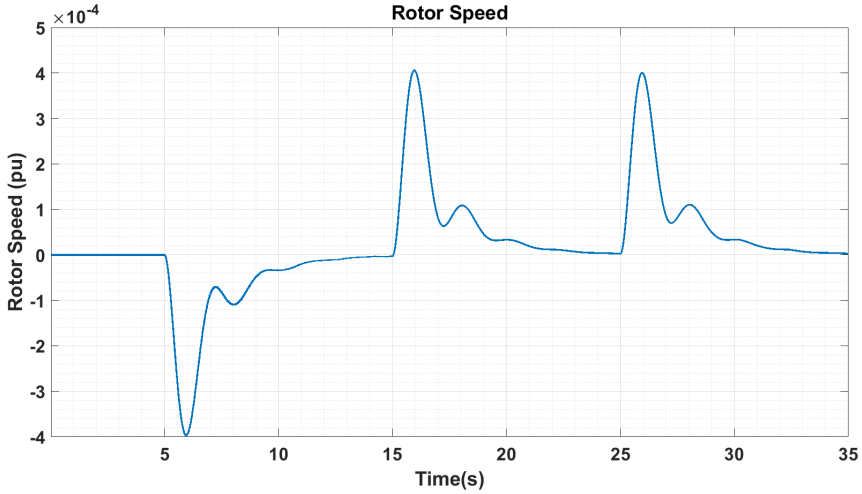

Figure 4.9: The VFT rotor speed at synchronous interconnection operation.

voltage magnitude, frequency and impedance, are adjusted according to the described scenario in the reference.

Table 4.5: Model Verification scenario base values[29].

Parameters	**Symbol**	**Value**	**Unit**
Nominal Power	S_{Base}	4150	VA
Nominal Line RMS Voltage	V_{Base}	400	V
Nominal Frequency	f_{Base}	50	Hz

Table 4.6: Model Verification scenario WRIM parameters[29].

Parameters	Symbol	Value	Unit
Stator Resistance	R_s	0.01965	pu
Stator Reactance	X_s	0.0397	pu
Rotor Resistance	R_r	0.01965	pu
Rotor Reactance	X_r	0.0397	pu
Mutual Reactance	X_m	1.895	pu
Inertia Constant	H	14.96	pu
Friction Factor	D	0.01	pu
Pole Pairs	P_p	4	

Table 4.7: Model Verification scenario tie-in parameters[29].

Parameters	Symbol	Value	Unit
Stator Connected Capacitor Bank	B_1	1600	VAR
Rotor Connected Capacitor Bank	B_2	1600	VAR
Grid#1 Line-Line RMS Voltage	$V_{LL-RMS1}$	1	pu
Grid#1 Equivalent Reactance	X_{G1}	0.03	pu
Grid#2 Line-Line RMS Voltage	$V_{LL-RMS2}$	1	pu
Grid#2 Equivalent Reactance	X_{G2}	0.03	pu

4.3.2 Active Power Transfer Magnitude and Direction Impact on The Reactive Power Flow Characteristic

In this case, both girds' voltage magnitude is constantly maintained at 1(pu) while the active power transfer order from grid#1 to grid#2 changes from 1(pu) to -1(pu) to investigate the active power transfer magnitude and direction impact on the reactive power flow. Complete Matlab\Simulink reports of this scenario simulation and analytical calculation are in appendices C and D.

Figure 4.10 shows the derived reactive power characteristic from the developed model, and Figure 4.11 shows the reactive power characteristic published in [29]. Comparing the two graphs proves that the developed model accurately measures the reactive power consumption by the VFT and reactive power flow from both grids based on the model parameters and successfully derives the reactive power characteristic. The minor deviations from the reference are because of the uncontrolled voltage on the VFT's stator and rotor in this study, unlike the reference research that kept the voltage at 1(pu). Also, it can be noticed from reactive power flow magnitudes at zero active power transfer that the exact value for capacitor banks in this specific scenario in [29] is different from the general mentioned value, the 77(pu) in total. However, this study uses the general capacitor banks values for the model verification scenario simulation due to the lack of clarification in the reference.

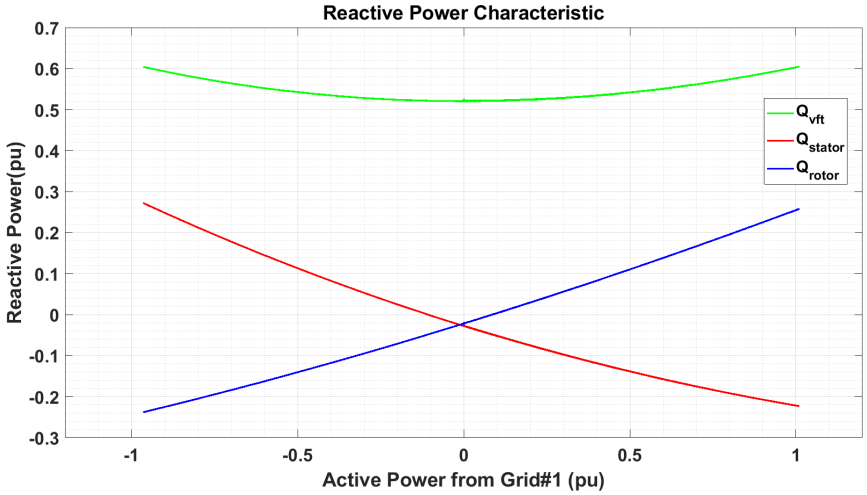

Figure 4.10: Model verification scenario reactive power characteristic with varying active power transfer.

The expressed analytical study in section 2.4 is also implemented in Matlab to investigate the model's correctness. Figure 4.12 shows the result for both analytical calculation and the Simulation result. It also proves that the simulation correctly measures the reactive power flow and successfully derives the reactive power characteristic. The deviations between the simulation result and analytical calculation are the product of more simplification and linearization, such as neglecting VFT's stator and rotor voltage deviation with power transfer order variation in the analytical calculation.

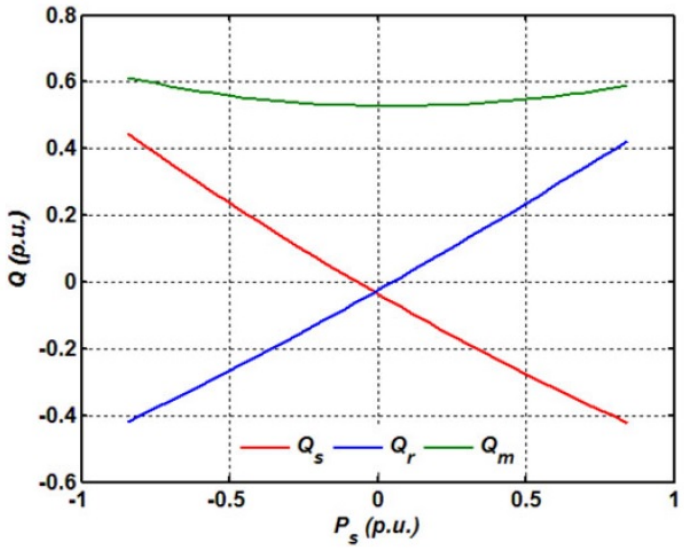

Figure 4.11: Model Verification reference reactive power characteristic with varying active power transfer[29].

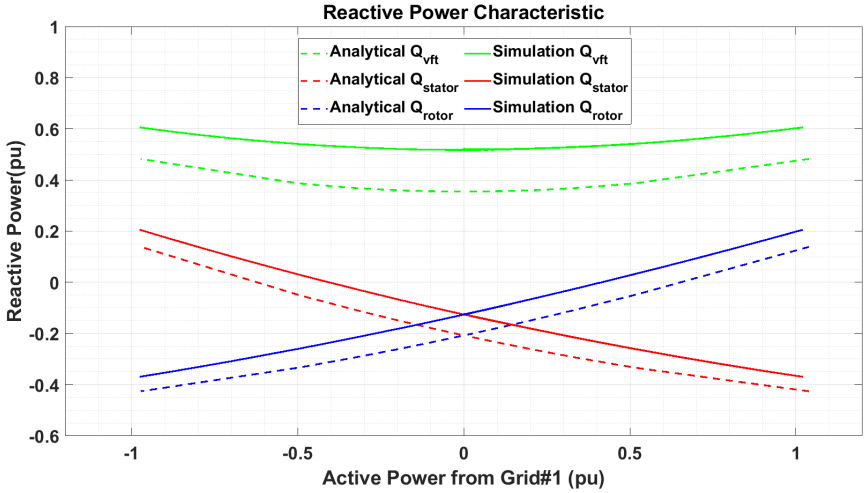

Figure 4.12: Model verification analytical calculated reactive power characteristic with varying active power transfer.

4.3.3 Grid Voltage Deviation Impact on The Reactive Power Flow Characteristic

In this case, the power transfer order is constat at 0.85(pu) from grid#1 to grid#2 in one scenario, and vice versa in the other, at the same time grid#1 voltage is constantly maintained at 1(pu). In contrast, grid#2 voltage varies $\pm$6% from the nominal value in both scenarios to investigate one grid voltage variation impact on the reactive power flow. Complete Matlab\Simulink report of

these two scenario simulations exists in appendix E

Figure 4.13 shows the obtained reactive power characteristics from the developed model, and Figure 4.14 shows the reactive power characteristics published in [29]. Evaluating the obtained reactive power flow with the reference ones indicated that the model is working correctly with some differences from the reference research model. The main difference that causes deviation in results, as mentioned before in subsection 4.3.2 is uncontrollable VFT's stator and rotor voltages in the developed model. The unregulated voltage on VFT buses affects reactive power flow through the WRIM. At the same time, one of the negative impacts of the reactive power flow is undesired voltage change.

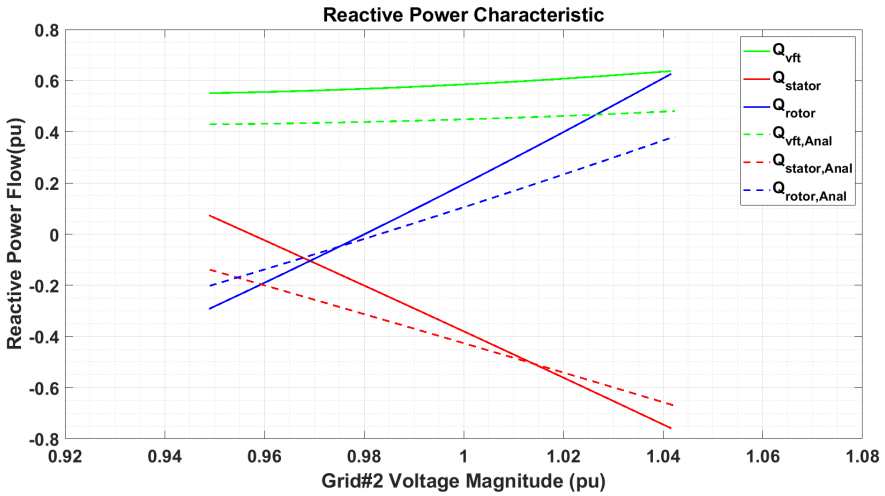

(a) 0.85(pu) Active power transfer from Grid#1 to Grid#2.

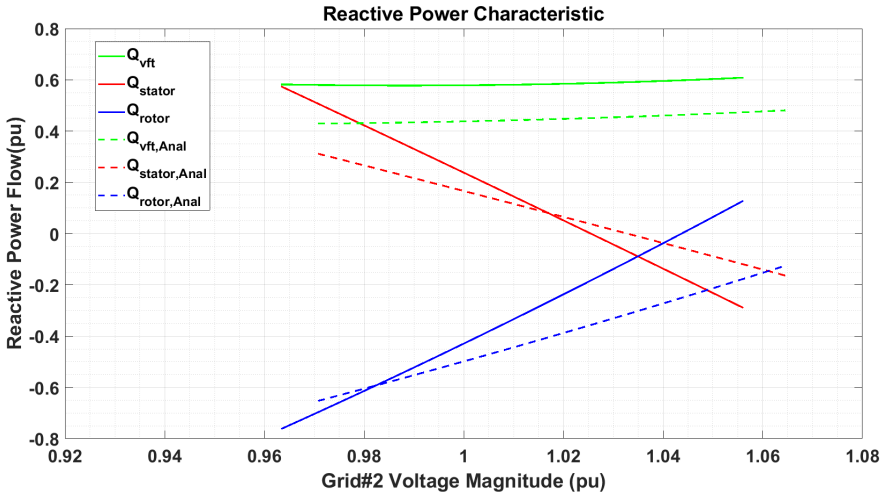

(b) 0.85(pu) Active power transfer from Grid#2 to Grid#1.

Figure 4.13: Model verification reactive rower characteristic with Grid#2 voltage variation.

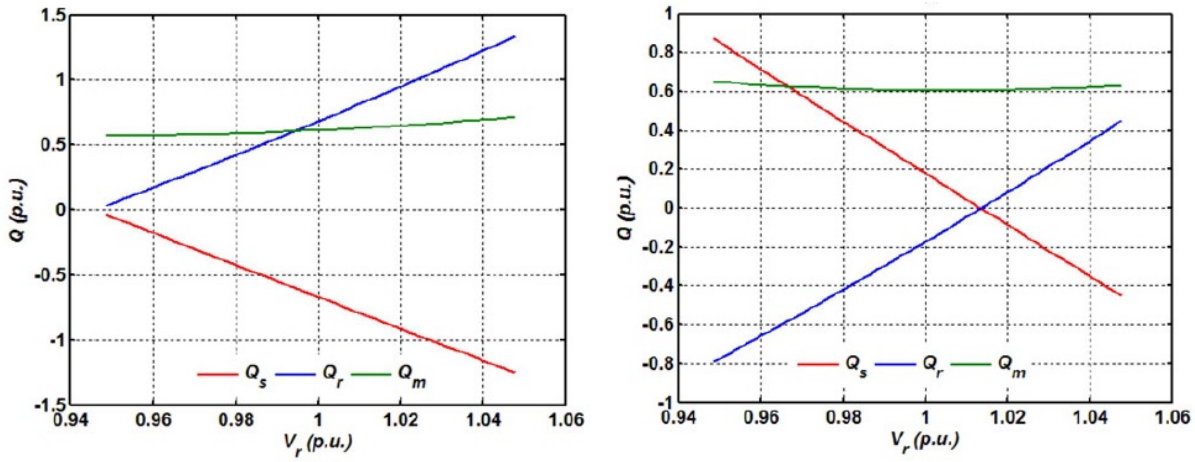

(a) 0.85(pu) Active power transfer from stator to rotor. **(b)** 0.85(pu) Active power transfer from rotor to stator.

Figure 4.14: Model verification reference reactive power characteristic with a grid voltage variation[29].

Chapter 5

Discussion

This chapter defines different simulation scenarios and each scenario operating condition. It represents the scenarios simulation results, including the reactive power flow characteristic and maximum possible active power transfer in the defined interconnection condition and the VFT response to a frequency disturbance event. It discusses the VFT limits and requirements for frequency shifting operation and frequency ancillary service.

5.1 VFT Asynchronous Interconnections Operating Condition

In this section, different VFT interconnection operating conditions used in the test system to investigate the VFT behaviour are explained.

5.1.1 X-rotor Power Take-off System

X-rotor offshore wind turbine concept aims to cut the offshore wind's energy cost. This new offshore turbine suggests reducing investing capital, operation and maintenance costs compared to all four standard types of wind turbines. Cost analysis shows the potential of saving up to 55% of O&M costs and up to 32% of capital costs. This potential offers the possibility of reducing LCoE up to 26% by combining capital and O&M costs saving. X-rotor offshore wind turbine is a new radical hybrid concept of HAWT, and VAWT [2].

The main rotor, the vertical rotor, helps energy capturing and increases wind speed considerably on the secondary rotor, the horizontal rotor. Preventing power take-off from the main rotor eliminates the high torque power train requirements in the VAWTs. Also, the high-speed wind on the second rotor facilitates a direct drive train for power generation. This configuration results in a more straightforward, lighter and cheaper power take-off train. Still, the X-rotor power take-off system requires a rotary power transmitter from the main rotor to the stationary part of the turbine. It should also handle the oscillation in electrical frequency induced by the inherent oscillating wind speed on the secondary rotor even in a constant wind profile [44].

The X-rotor offshore wind turbine included two suggested generators at 2.5(MW) rated power with the rated line voltage of 33(kV)[44]. The power take-off system nominal electrical frequency, considering the nominal X-rotor operating frequency of 25(Hz), [2], with 4 poles pairs generators, is 50(Hz). [44] suggests 10% oscillation in the secondary rotors rotational mean speed amplitude at 5(m/s) wind speed, 20% at wind speed of 10(m/s) and 40% at 20(m/s) wind speed. Considering the rated wind speed f 12.66(m/s), the mean rotational speed or nominal frequency of the generated power will oscillate with 25.32%. The frequency operating range of the X-rotor power take-off system VFT is 37.34(Hz) to 62.66(Hz). Table 5.1 shows the X-rotor power take-off VFT parameters.

The GE 100(MW) VFT system electrical parameters included the stator and rotor resistances and reactances, magnetising reactance, damping or friction factor and inertia constant introduced in per-unit that helps to keep them the same in different base values in various VFT applications. The machine number of pole pairs also introduced the same.

In this case, the Grid#2 assumed as the stationary side of the X-rotor power take-off RT and the Grid#1 taken as the X-rotor turbine and the wind farm collector PCC. The wind farm in-

Table 5.1: X-rotor power take-off system parameters.

Parameters	**Symbol**	**Value**	**Unit**
Nominal Power	S_{Base}	6	MVA
Nominal Line RMS Voltage	V_{Base}	3.3	kV
Nominal Frequency	f_{Base}	50	Hz
Minimum Frequency	f_{min}	37.34	Hz
Maximum Frequency	f_{max}	62.66	Hz
Stator Connected Capacitor Bank	B_1	528	KVAR
Rotor Connected Capacitor Bank	B_2	528	KVAR
X-rotor RT Line-Line RMS Voltage	$V_{LL-RMS1}$	1	pu
X-rotor RT Equivalent Resistance	R_{g1}	0.002	pu
X-rotor RT Equivalent Reactance	X_{g1}	0.1194	pu
Turbine PCC Line-Line RMS Voltage	$V_{LL-RMS2}$	1	pu
Turbine PCC Equivalent Resistance	R_{g2}	0.00664	pu
Turbine PCC Equivalent Reactance	X_{g2}	0.0664	pu

ternal grid is assumed to be a weak grid with an SCR of 10 and a X/R ratio of 10. And the X-rotor power train resistance and reactances are calculated for two 2.5(MW) permanent magnet synchronous generators (PMSG) and a 5(MW) rotary transformer. With the described configuration, the power transfer direction is only from the Grid#2 to the Grid#1. And the Grid#1 frequency is constantly on 50(Hz), and the Grid#2 frequency oscillates between 37.34(Hz) to 62.66(Hz).

5.1.2 LFAC Power Transmission For OWFs

The LFAC system expands the power transmission capacity of an HVAC link by reducing the charging current in the transmission line. Lower reactive power generating at lower frequency increasing active power transmission capacity [8]. Additionally, decreasing inductive reactance of HVAC links by lowering the operating frequency, reducing the reactive power flow in the line and consequently increasing the active power transmission capacity [9].

The low-frequency AC (LFAC) system utilises railway systems in many countries such as Norway, Germany and the US for almost a century. The railway system in these European countries uses 16.7(Hz) (50/3(Hz)), and some train systems in the US operate at 25(Hz) [7]. Some ref-

erences suggest different operating frequencies for the LFAC system from 16.7(Hz), 20(Hz) and 25(Hz), which this study goes with traditional value for the European railway system [7]. Offshore HVAC links for offshore wind power transmission parameters extracted from [6] and converted to per unit values to use in this study.

On the other side, recent massive constructed offshore wind turbines with rotor diameters of 220(m) operate at a very low rotor speed around 7(RPM) to 12(RPM) [10]. Considering their direct-drive power trains and presuming a four-pole pairs generator utilise the turbine, The electrical frequency of the power generated is something around 0.5(Hz). This value is not practical because the enormous transformer volume required in the wind turbine refers to the core cross-section relation with the operating frequency. Also, hand calculation shows a super high reactive power flow that does not make sense to investigate. But it is possible to take 5(Hz) as an extreme working condition for the VFT system and examine the VFT power flow behaviour in the range of 5(Hz) to 27(Hz), around 65% of frequency deviation from the selected operating frequency of the LFAC system. Table 5.2 shows the VFT parameters in the LFAC power transmission system for OWF.

Table 5.2: LFAC system parameters in power transmission from OWF.

Parameters	**Symbol**	**Value**	**Unit**
Nominal Power	S_{Base}	100	MVA
Nominal Line RMS Voltage	V_{Base}	17	kV
Nominal Frequency	f_{Base}	16.7	Hz
Minimum Frequency	f_{min}	5.2	Hz
Maximum Frequency	f_{max}	27.2	Hz
LFAC HVAC Link Line-Line RMS Voltage	$V_{LL-RMS1}$	1	pu
LFAC HVAC Link Equivalent Resistance	R_{g1}	0.0165	pu
LFAC HVAC Link Equivalent Reactance	X_{g1}	0.04125	pu
OWF PCC Line-Line RMS Voltage	$V_{LL-RMS2}$	1	pu
OWF PCC Equivalent Resistance	R_{g2}	0.00664	pu
OWF PCC Equivalent Reactance	X_{g2}	0.0664	pu

In this case, the Grid#2 assumed as the offshore wind farm point of common connection and the Grid#1 taken as the HVAC transmission link for the LFAC system. The wind farm internal grid is assumed to be a weak grid with an SCR of 10 and a X/R ratio of 10. And the offshore HVAC transmission line resistance and reactances are calculated for 150(km) HVAC link according to suggested parameters from [6]. With the described configuration, the power transfer direction is only from the Grid#2 to the Grid#1. And the Grid#1 frequency is constantly on 16.7(Hz), and

the Grid#2 frequency oscillates between 5.2(Hz) to 27.2(Hz).

5.1.3 Grid Interconnections

The asynchronous grid interconnection parameters and operating conditions are the same as defined in the 4.1.2. To cover all possible future operatings, the test frequency deviation range is determined $\pm$50% for both 50 (Hz) and 60(Hz).

5.1.4 Combined ESB and VFT as Synchronous Power Generator

The employed parameter values for the ESB bank combined with the VFT for frequency ancillary services are the same as defined values in the 4.1.2. The system's base operating frequency is 60(Hz), equal to the VFT system reference value in the Langlois substation. The grid#1 assumed the ESB side, and the grid#2 side assumed the weak grid. In this scenario, first, a 0.85(pu) load is connected to the grid#2 side at 1(second), and after 5(seconds), the power source in the grid#2 is lost. The grid#1 or the ESB and the VFT continue delivering power to the 0.85(pu) and operate as an islanded power system.

5.2 VFT Characteristics

This section represents and analysis the different scenarios' simulation results.

5.2.1 X-rotor Power Take-off System

Figure 5.1 depicts the maximum possible active power take-off from the X-rotor offshore wind turbine. It shows that almost in the whole range of X-rotor rated operating, it is possible to take power from the turbine, but with a deficient power factor at the operating frequency edges. The reasonable range for power take-off with PF higher than 80% is between 43(Hz) and 62(Hz).

5.2.2 LFAC Power Transmission Form OWFs

Figure 5.2 depicts the maximum possible active power transmission through the VFT in the defined LFAC system. It shows the VFT system is not practical at all at the operating frequencies of OWF lower than 13(Hz) and over the 21(Hz). The reasonable operating PF for the system is

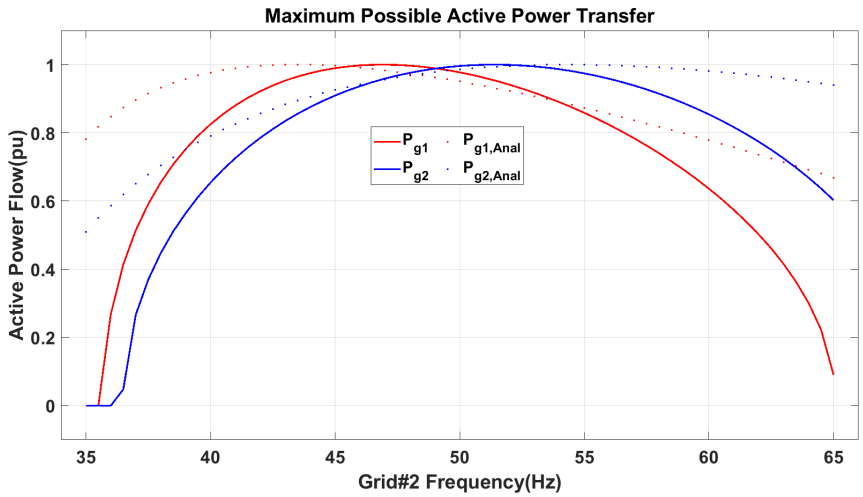

Figure 5.1: The VFT maximum possible active power transfer during frequency shifting in X-rotor power take-off system.

even narrower between 14(Hz) and 19(Hz) at the PF of 80%.

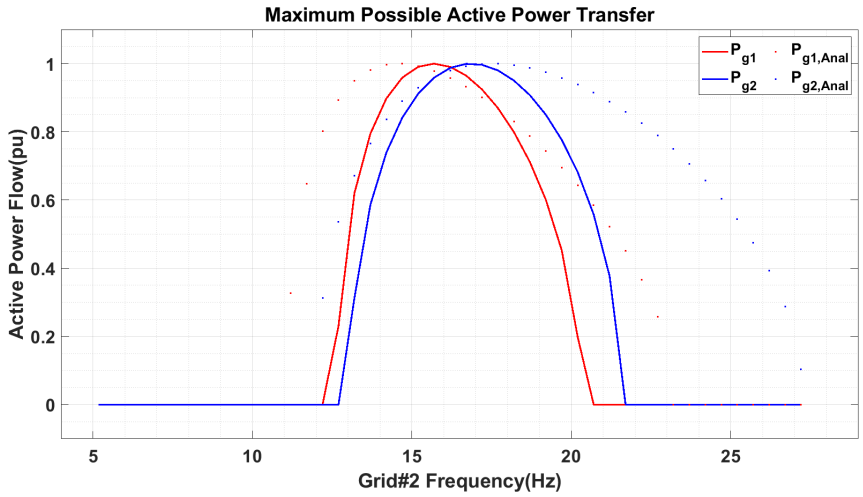

Figure 5.2: The VFT maximum possible active power transfer during frequency shifting in LFAC power transmission system from OWFs.

5.2.3 Grids Interconnection

Figure 5.3 depicts the maximum possible active power transmission with the VFT asynchronous grids interconnection. It shows the 50(Hz) rated interconnection transfer power between 38(Hz)

and 64(Hz), and it is between 46(Hz) and 76(Hz) for the 60(Hz) rated VFT interconnection. The above 80% power factor for 50(Hz) interconnection is 42.5(Hz) and 57.5(Hz), and for the 60(Hz) rated VFT is between 51(Hz) and 70(Hz).

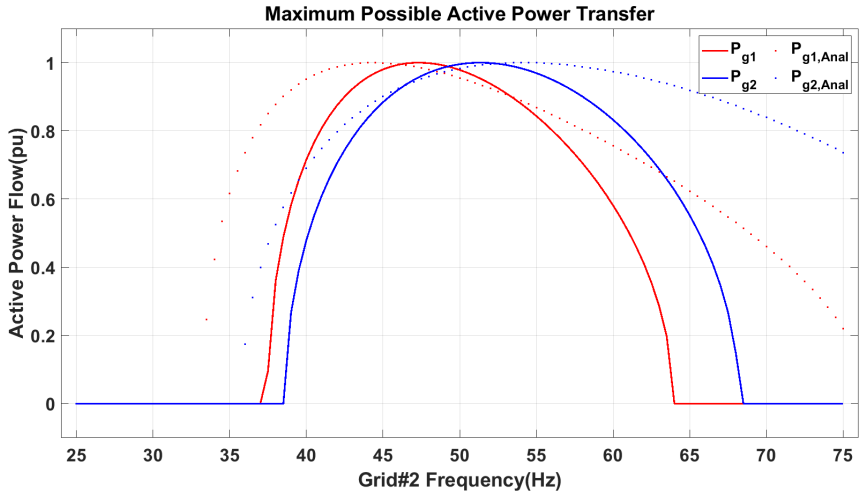

(a) 50(Hz) Operating frequency.

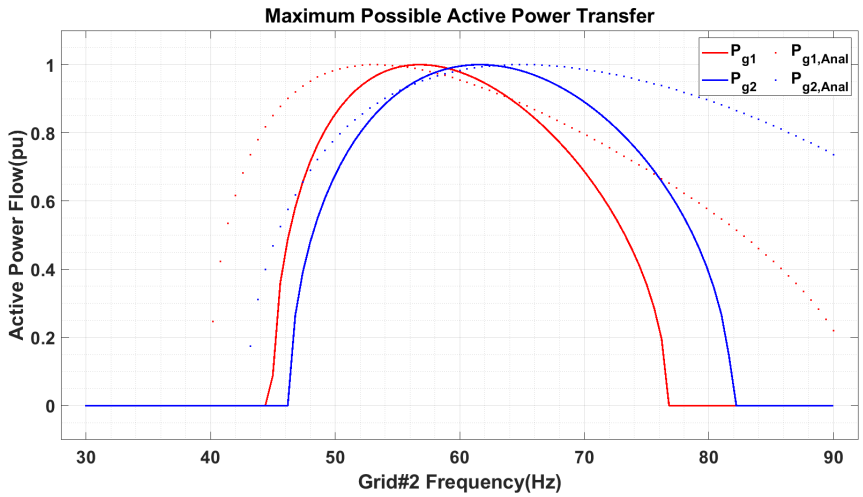

(b) 60(Hz) Operating frequency.

Figure 5.3: The VFT power maximum possible active power transfer during frequency shifting in asynchronous grids interconnection.

Comparing the simulation results for the different scenarios in per-unit values shows that the maximum possible power transmission based on the VFT's reactive power requirement is better in stronger grids interconnections. Otherwise, operating at the higher-rated frequency offer a more comprehensive range of absolute frequency deviation.

5.2.4 Combined ESB and VFT as Synchronous Power Generator

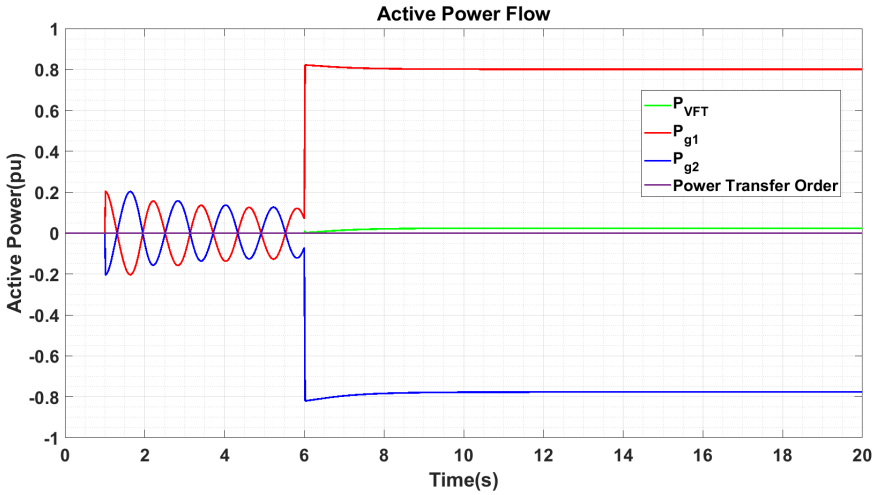

Figure 5.4: The VFT active power flow in frequency disturbance.

Figure 5.9 illustrates the power demand change in the power system over time. It shows the rotor swing effect from second 1, when the 0.85(pu) load is connected to the *grid*#2. It is noticeable that the VFT inertia's damping the swing oscillation of 0.67(Hz). Figure 5.5 shows at the second 6 when the system loses the grid#2 power source, and the ESB and the VFT operate in islanded mode, the system experience a RoCoF of 0.675(Hz/sec) or 0.01125(pu/sec). The testing VFT system with an inertia constant of 25(pu-sec) at the 0.85(pu) power demand change event, is expected to have 0.017(pu/sec) RoCoF. The difference could result from pre 5 seconds load sharing with the grid#2 and not exactly 0.85(pu) effective load change experience by the VFT. The grid#2 frequency settled at 0.9735(pu) or 58.41(Hz).

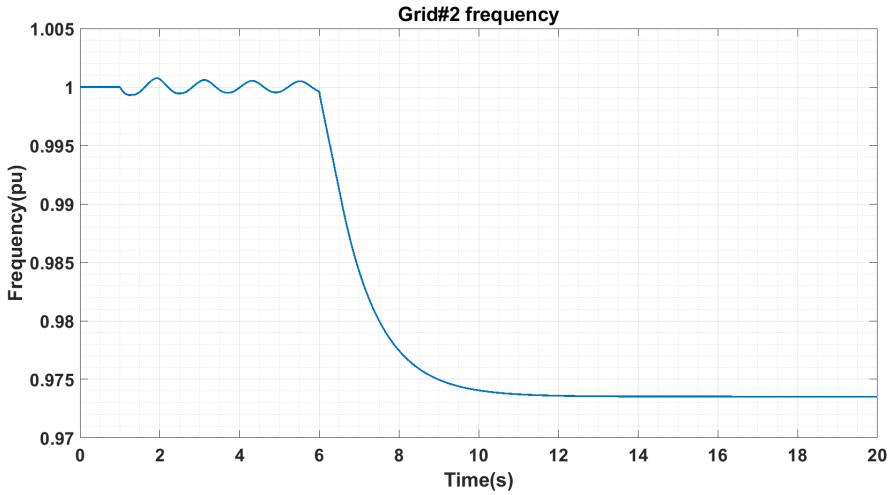

Figure 5.5: The VFT frequency response at the gird#2 side with frequency disturbance.

5.3 Voltage Stability

5.3.1 Frequency Shifting Voltage Stability

The VFT interconnection voltage analysis shows the acceptable voltage stability, not exceeding ∓ 0.1(pu), if the system operates with a power factor greater than 80%. The operating range without any voltage regulator or multi-stage reactive power compensators is remarkable.

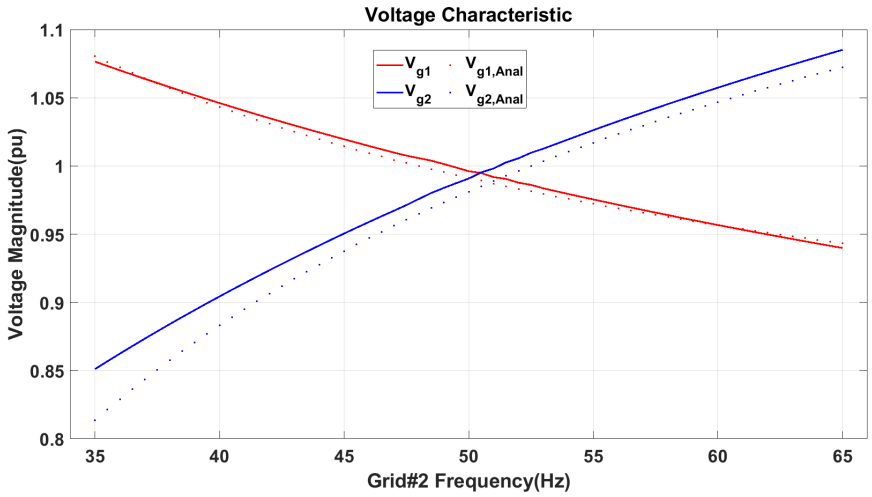

Figure 5.6: The VFT voltage characteristic during frequency shifting in X-rotor power take-off system at 1(pu) active power delivery from the turbine.

Voltage stability discussion in OWF LFAC system.

Voltage stability in asynchronous grids interconnection.

5.3.2 Frequency ancillary service Voltage Stability

The combined system voltage stability also shows an acceptable range and does not exceed 0.1(pu) deviation.

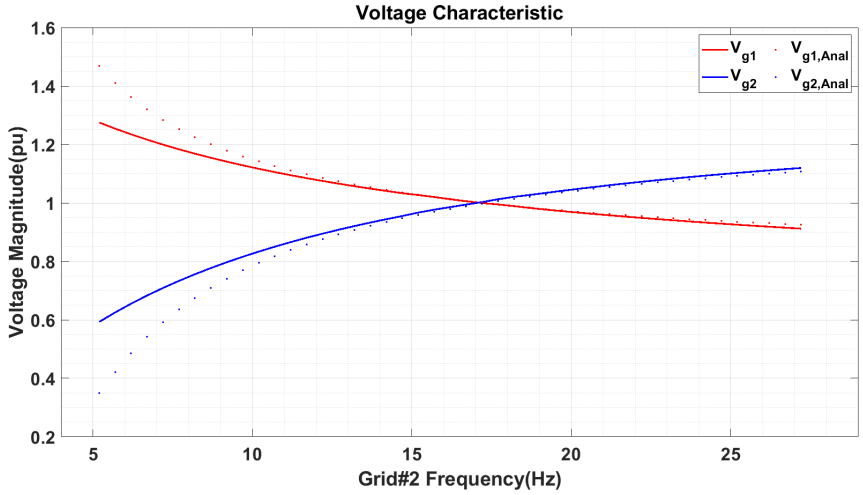

Figure 5.7: The VFT voltage characteristic during frequency shifting in LFAC power transmission system at 1(pu) active power delivery from the OWF.

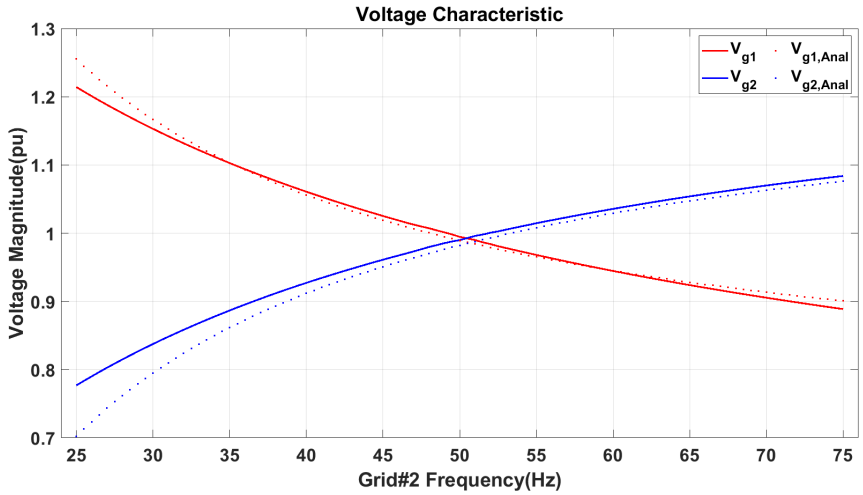

(a) 50(Hz) Operating frequency.

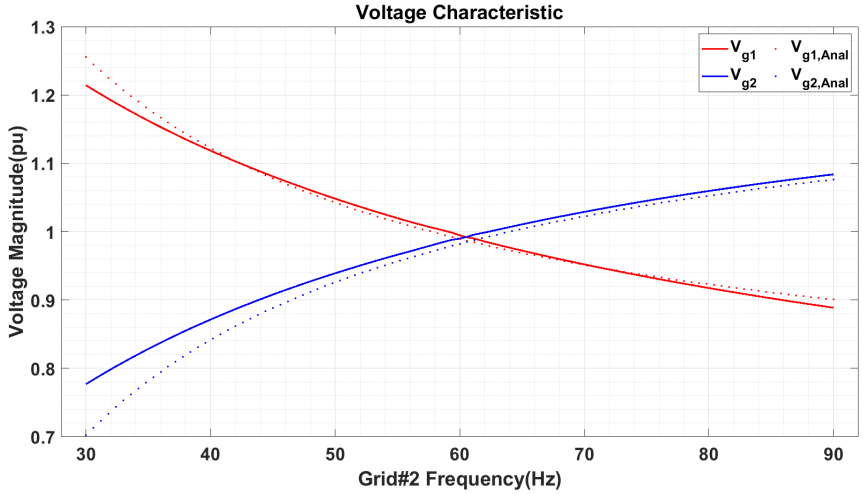

(b) 60(Hz) Operating frequency.

Figure 5.8: The VFT voltage characteristic during frequency shifting in asynchronous grids interconnection at 1(pu) active power transfer from the grid2.

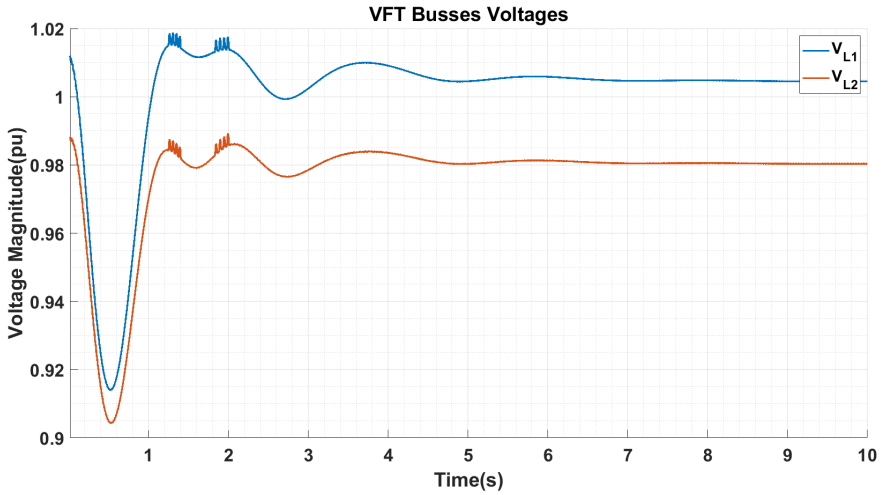

Figure 5.9: The Voltage at VFT busses during frequency disturbance.

Chapter 6

Conclusion and Future Work

This chapter concludes the performed study derived results considering the specified motivation and objectives and suggests relevant future work for further investigations, which this study excluded.

6.1 Conclusion

This study tested the VFT asynchronous interconnection in four scenarios and operating conditions. It shows the maximum possible active power transfer through a VFT interconnection would improve by connecting to a stronger grid with less voltage influenced by the power flow. It suggests employing the VFT system with a higher operating frequency rate offer a wider absolute frequency shifting range. It also helps to reduce the VFT size, considering the required cross-section magnetic core is smaller for the higher frequencies. This study shows that the VFT system is not a promising technology for LFAC power transfer according to the hug constructed induction machine and narrow practical frequency shifting range. For standard grid interconnection, 50(Hz) and 60(Hz), introducing voltage regulators and power factor improvement would be a reasonably acceptable asynchronous grid interconnections solution.

On the other side, the ESB combined with a VFT offers a synchronous power generation plant characteristic for frequency ancillary services. This study reviewed the possible frequency control levels it can suggest. The test result of RoCoF at 0.01125(pu/sec) and analysis of 0.017(pu/sec), which is significantly lower than the acceptable range from the grid code represented in Table 3.2. Also, natural rotor swing damping response without any additional proposed control function suggest a general power system stability improvement. The combined ESB with a VFT, theoretically and partially tested, indicates stage I, II, III and IV frequency ancillary services potential. It also enhances the power operating reliability with the bidirectional power transfer possibility, which absorbs the surplus power mismatch in the grid to charge the ESB. It prevents the sudden power rejection problem by losing transmission lines.

6.2 Future Work

This study excluded many aspects of stability analysis in the VFT interconnection and simplified many parts of the tested systems. Some likely future works that would help more accurate analysis of the VFT asynchronous interconnection and the combined ESB and VFT as a synchronous power generating plant, stability and potential ancillary services are:

-Examine the voltage stability and regulation in the VFT interconnection system.

-Implement practical control loops to the test model, such as the DC motor drive control, which is similar to the governor control design of the synchronous power generation plants.

-Introduce a more comprehensive grid including other power generation plants and more realistic loads.

-Study the VFT interconnection rotor swing damping.

-Conduct a modal analysis of the comprehensive grid model and investigate the VFT impact on the grid stability.

-Study different ESB technologies and their cons and pros in combination with the VFT system.

References

[1] K. Nasrollahi, Anaya-Lara, Olimpo. "Modelling and Analysis of a Rotary Transformer for Power Take-off System of a X-Rotor Wind Turbine", June 2021

[2] Leithead, William; Camciuc, Arthur; Amiri, Abbas Kazemi; Carroll, James, "The X-Rotor Offshore Wind Turbine Concept" in *Journal of physics*, Conference series, 2019-10-01, Vol.1356 (1), p.12031

[3] Schutte, T., Gustavsson, B. and Strom, M. (2001) "The use of low frequency AC for offshore wind power." in *Proceedings of the Second International Workshop on Transmission Networks for Offshore Wind Farms* (ed T. Ackermann), Royal Institute of Technology, Stockholm.

[4] Yang, Jian, et al. “Applicability of Low Frequency Transmission Technology in Offshore Wind Power Transmission Scene.” in *E3S Web of Conferences*, vol. 182, 2020, p. 1001.

[5] Dakic, Jovana, et al. “Low Frequency AC Transmission Systems for Offshore Wind Power Plants: Design, Optimization and Comparison to High Voltage AC and High Voltage DC.” in *International Journal of Electrical Power Energy Systems*, vol. 133, 2021, p. 107273.

[6] Hao Chen, et al. “Low-Frequency AC Transmission for Offshore Wind Power.” in *IEEE Transactions on Power Delivery*, vol. 28, no. 4, 2013, pp. 2236–2244.

[7] Pfeiffer, A, et al. “Modern Rotary Converters for Railway Applications.” in *Proceedings of the 1997 IEEE/ASME Joint Railroad Conference*, 1997, pp. 29–33.

[8] Song-Manguelle, Joseph, et al. “Power Transfer Capability of HVAC Cables for Subsea Transmission and Distribution Systems.” in *IEEE Transactions on Industry Applications*, vol. 50, no. 4, 2014, pp. 2382–2391.

[9] Ruddy, Jonathan, et al. “Low Frequency AC Transmission for Offshore Wind Power: A Review.” in *Renewable Sustainable Energy Reviews*, vol. 56, 2016, pp. 75–86.

[10] General Electric offshore wind turbine Haliade-series 6MW-14MW technical datasheet, available on *https://en.wind-turbine-models.com/turbines/2320-ge-general-electric-haliade-x-14-mwdatasheet*

[11] Yun,W.C.; Zhang, Z.X., "Electric power grid interconnection in Northeast Asia." in *Energy Policy* 2006, 34, 2298–2309.

[12] Ongsakul,W.; Teng, K.; Marichez, S.; Jiang, H., "An innovation idea for energy transition towards sustainable and resilient societies: Global energy interconnection." in *Glob. Energy Interconnect.* 2018, 1, 312–318.

[13] David Elliott, "Emergence of European supergrids – Essay on strategy issues" in *Energy Strategy Reviews*,Volume 1, Issue 3,2013,Pages 171-173,ISSN 2211-467X

[14] Zhang, X., Lu, C., Liu, S., Wang, X. (2016). "A review on wide-area damping control to restrain inter-area low frequency oscillation for large-scale power systems with increasing renewable generation." in *Renewable and Sustainable Energy Reviews*, 57, 45-58.

[15] Attya, A.B, O. Anaya-Lara, and W.E Leithead. "Novel Concept of Renewables Association with Synchronous Generation for Enhancing the Provision of Ancillary Services." in *Applied Energy* 229 (2018): 1035-047.

[16] Attya, A. B., and Olimpo Anaya-Lara. "Provision of frequency support by offshore wind farms connected via HVDC links." in *5th IET International Conference on Renewable Power Generation (RPG)* 2016. IET, 2016.

[17] B. Bagen, D. Jacobson, G. Lane, and H. M. Turanli, “Evaluation of the performance of backto-back HVDC converter and variable frequency transformer for power flow control in a weak interconnection,” in *IEEE Power Engineering Society General Meeting*, PES, 2007.

[18] J. Marczewski, “VFT Applications Between Grid Control Areas,” in *IEEE Power Engineering Society General Meeting*, 2007.

[19] Imdadullah, Alamri B, Hossain MA, Asghar MSJ. , "Electric Power Network Interconnection: A Review on Current Status, Future Prospects and Research Direction." in *Electronics.* 2021; 10(17):2179. https://doi.org/10.3390/electronics10172179

[20] Byeonghyeon An et al, "Economical Comparisons of Interconnection Technology for Asynchronous AC Power Grids" in *2019 J. Phys.: Conf. Ser. 1304 012009*

[21] M. M. Khan, Imdadullah, J. Nebhen and H. Rahman, "Research on Variable Frequency Transformer: A Smart Power Transmission Technology," in *IEEE Access, vol. 9, pp. 105588-105605,* 2021, doi: 10.1109/ACCESS.2021.3099747.

[22] Merkhouf, A ; Doyon, P ; Upadhyay, S, "Variable Frequency Transformer—Concept and Electromagnetic Design Evaluation" in *IEEE transactions on energy conversion*, 2008-12, Vol.23 (4), p.989-996

[23] E. Larsen, “A classical approach to constructing a power flow controller,” in *IEEE Power Eng. Soc. Summer Meet.*, vol. 2, pp. 1192–1195, 1999.

[24] R. Gauthier. (2004, Nov.). "A world-first VFT installation in quebec. Transm. Distrib. World [Online]." available on *http://tdworld.com/mag/power_worldfirst_vft_installaton*

[25] P. Doyon, D. McLaren, M. White, Y. Li, P. Truman, E. Larsen, C.Wegner, E. Pratico, and R. Piwko, “Development of a 100 MW variable frequency transformer,” presented at Canada Power, Toronto, ON, Canada, Sep. 28–30, 2004.

[26] R. J. Piwko, E. V. Larsen and C. A. Wegner, "Variable frequency transformer - a new alternative for asynchronous power transfer," in *2005 IEEE Power Engineering Society Inaugural Conference and Exposition* in Africa, 2005, pp. 393-398, doi: 10.1109/PESAFR.2005.1611852.

[27] A. Merkhouf, S. Upadhyay and P. Doyon, "Variable frequency transformer - an overview," in *2006 IEEE Power Engineering Society General Meeting*, 2006, pp. 4 pp.-, doi: 10.1109/PES.2006.1709639.

[28] GE Energy "Variable Frequency Transformers - Grid Inter-tie" available on *https://www.gegridsolutions.com/products/brochures/powerd_vtf/vft_brochure.pdf*

[29] B. B. Ambati and V. Khadkikar, "Variable Frequency Transformer Configuration for Decoupled Active-Reactive Powers Transfer Control," in *IEEE Transactions on Energy Conversion*, vol. 31, no. 3, pp. 906-914, Sept. 2016, doi: 10.1109/TEC.2016.2550558.

[30] J. Bumby, J. Machowski, and J. W. Bialek, *Power System Dynamics: Stability and Control*, 2nd ed. Chichester, U.K.: Wiley, 2008

[31] F. I. Bakhsh, M. Irshad and M. S. J. Asghar, "Modeling and simulation of variable frequency transformer for power transfer in-between power system networks," in *India International Conference on Power Electronics 2010 (IICPE2010)*, pp. 1-7, doi: 10.1109/IICPE.2011.5728119.

[32] J. A. Melkebeek, *Electrical Machines and Drives: Fundamentals and Advanced Modelling*, Springer International Publishing AG, 2018

[33] D.Mc.Nabb,D.Nadeau, A.Nantel, E.Pratico, E.Larsen, G.Sybille, Van Que Do, D.Paré, "Transient and Dynamic Modeling of the New Langlois VFT Asynchronous Tie and Validation with Commissioning Tests" in *International Conference on Power Systems Transients*, Montreal, Canada on June 2005

[34] E.Pratico, C.Wegner, E.Larsen, R.Piwko, D.Wallace, D.Kidd, , "VFT Operational Overview – The Laredo Project" in *IEEE PES General Meeting*, Tampa, 2007

[35] Bush,R., Wolf,G. "The bulk power grid seeks intelligent operation." in *Transmission Distribution World*, 2006 58(12), S4-S7. Retrieved from https://www.proquest.com/trade-journals/bulk-power-grid-seeks-intelligent-operation/docview/211148224/se-2?accountid=12870

[36] Bortoni, Edson, et al. “The Benefits of Variable Speed Operation in Hydropower Plants Driven by Francis Turbines.” in *Energies (Basel)*, vol. 12, no. 19, 2019, p. 3719.

[37] Bajaj, Mohit, and Amit Kumar Singh. “Grid Integrated Renewable DG Systems: A Review of Power Quality Challenges and State-of-the-Art Mitigation Techniques.” in *International Journal of Energy Research*, vol. 44, no. 1, 2020, pp. 26–69.

[38] Ambati, Bharath Babu, et al. “A Hierarchical Control Strategy With Fault Ride-Through Capability for Variable Frequency Transformer.” in *IEEE Transactions on Energy Conversion*, vol. 30, no. 1, 2015, pp. 132–141.

[39] Wang, Li, and Long-Yi Chen. “Reduction of Power Fluctuations of a Large-Scale Grid-Connected Offshore Wind Farm Using a Variable Frequency Transformer.” in *IEEE Transactions on Sustainable Energy*, vol. 2, no. 3, 2011, pp. 226–234.

[40] Chen G, Zhou X, Chen R. "Variable frequency transformers for large scale power systems interconnection: theory and applications." John Wiley Sons; 2018 Jul 4.

[41] Ackermann, Thomas. " in Power Systems." 2nd ed., Wiley, 2012.

[42] N.P. W. Strachan, D. Jovcic, "Stability of a Variable-Speed Permanent Magnet Wind Generator With Weak AC Grids" in *IEEE TRANSACTIONS ON POWER DELIVERY*, VOL. 25, NO. 4, OCTOBER 2010

[43] Asynchronous Machine Block Documentation in *https://se.mathworks.com/help/physmod/sps/powersys/ref/asynchronousmachine.html*

[44] D.C.Gaona, A.Stock, W.Leithead, O.Anaya-Lara, L.Morgan, "X-SHAPED RADICAL OFFSHORE WIND TURBINE FOR OVERALL COST OF ENERGY REDUCTION, Secondary rotors and power train design", Dec. 2021, University of Strathclyde

[45] F. Katiraei, R. Iravani, N. Hatziargyriou and A. Dimeas, "Microgrids management," in *IEEE Power and Energy Magazine*, vol. 6, no. 3, pp. 54-65, May-June 2008, doi: 10.1109/MPE.2008.918702.

[46] Yoldaş, Yeliz, et al. “Enhancing Smart Grid with Microgrids: Challenges and Opportunities.” in *Renewable Sustainable Energy Reviews*, vol. 72, 2017, pp. 205–214.

[47] Silde, and Anaya-Lara, Olimpo. "Assessing the Impact of Synthetic Inertia Controls in DFIG Wind Turbines on Small-Signal Stability", 2021.

[48] Seneviratne, Chinthaka, and C Ozansoy. “Frequency Response Due to a Large Generator Loss with the Increasing Penetration of Wind/PV Generation – A Literature Review.” in *Renewable Sustainable Energy Reviews*, vol. 57, 2016, pp. 659–668.

[49] Eriksson, Robert, et al. “Synthetic Inertia versus Fast Frequency Response: a Definition.” in *IET Renewable Power Generation*, vol. 12, no. 5, 2018, pp. 507–514.

[50] Attya, A.B, J.L Dominguez-Garcia, and O. Anaya-Lara. "A Review on Frequency Support Provision by Wind Power Plants: Current and Future Challenges." in *Renewable Sustainable Energy Reviews* 81 (2018): 2071-087.

[51] Statnett. "Nasjonal veileder for funksjonskrav i kraftsystemet (NVF)". In: July 2020. Chap. 14.

Appendix A

Hand Calculations

Appendix B

Base Scenario Simulation Matlab\Simulink Simulation Report

Appendix C

Matlab\Simulink Simulation Report of Active Power Transfer Magnitude and Direction Impact On Reactive Power Flow

Appendix D

Matlab Analytical Calculation Report of Active Power Transfer Magnitude and Direction Impact On Reactive Power Flow

Appendix E

Matlab\Simulink Simulation Report of One Grid's Voltage Variation Impact On Reactive Power Flow

Appendix F

The VFT Characteristic in X-rotor Power Take-off system Test Report

Appendix G

The VFT Characteristic in LFAC Power Transmission System From OWFs Test Report

Appendix H

The VFT Characteristic in 50Hz Asynchronous Power System Interconnection Test Report

Appendix I

The VFT Characteristic in 60Hz Asynchronous Power System Interconnection Test Report

Appendix J

The VFT System Response to the Frequency Disturbance